Science Objectives And Performance Of A Radiometer And Window Design For Atmostspheric Entry Experiments

Roger Craig
MCAT Institute
Moffett Field
California

5/26/93

DRAFT

SCIENCE OBJECTIVES AND PERFORMANCE OF A RADIOMETER AND WINDOW DESIGN FOR ATMOSPHERIC ENTRY EXPERIMENTS

ROGER A. CRAIG[1] , WILLIAM C. DAVY[2] AND ELLIS E. WHITING[3]

ABSTRACT

The Radiative Heating Experiment, RHE, aboard the Aeroassist Flight Experiment, AFE, (now cancelled) was to make in-situ measurements of the stagnation region shock layer radiation during an aerobraking maneuver from geosynchronous to low earth orbit. The measurements were to provide a data base to help develop and validate aerothermodynamic computational models. Although cancelled, much work was done to develop the science requirements and to successfully meet RHE technical challenges. This paper discusses the RHE scientific objectives and expected science performance of a small sapphire window for the RHE radiometers. The spectral range required was from 170 to 900 nm. The window size was based on radiometer sensitivity requirements including capability of on-orbit solar calibration. Window contamination from

---

[1] MCAT Institute
Work performed under NASA Cooperative Agreement NCC2-762
NASA Ames Research Center
Moffett Field, CA 94035

[2] Eloret Institute
Work performed under NASA Cooperative Agreement NCC2-XXX
1176 Maraschino Drive
Santa Clara, CA 94057

[3] Eloret Institute
Work performed under NASA Cooperative Agreement NCC2-XXX
1176 Maraschino Drive
Santa Clara, CA 94057

spacecraft material (volatiles or particulates) is a concern, especially for ultraviolet performance, and requires careful identification and control. The window described can withstand the aeropass heating pulse and maintain optical performance to meet the objectives.

I-INTRODUCTION

The advent of the Space Station Freedom will usher in a new capability for planetary exploration and utilization of Earth/moon space. Lunar and planetary mission vehicles could be assembled, deployed, and retrieved on this platform without ever returning to earth. New, efficient, space transportation systems are needed to exploit this capability. A promising technique is aeroassist-- an Aeroassisted Space Transportation Vehicle, ASTV, is a vehicle equipped with a lightweight, low L/D, forebody heatshield. An ASTV, returning from a mission, would need to decelerate and alter its orbital parameters to rendezvous with the space station. These orbital changes would be achieved during a pass through the upper atmospheric (figure G). By controlling pitch and roll, the forebody aerodynamic forces would be directed to exit the ASTV into the desired orbit. The STS could then provide the link with earth.

Aeroassist can reduce or eliminate the need to carry decelerating retro-rockets and their fuel on a mission. There is potential for substantially lower space transportation costs if light weight, efficient heat shields can be designed. The present capability for predicting the ASTV heat protection requirements is based on the present capability to model aerothermodynamic processes. These models are of necessity based on many approximations and need validation data to reduce uncertainties. This is especially true for predictions of the heat load from the shock layer radiation. These uncertainties need to be resolved before we can design heat shields with minimum conservatism to degrade the benefits.

A NASA Aerocapture Technology Working Group was formed in 1980 to meet this challenge. This group identified specific technical issues which must be addressed to develop the design capability for routine use of aeroassist to modify orbits. The group agreed that a technical data base from a flight experiment was required. This data base would be used to improve and validate computational models which would form the basis for ASTV design codes. Radiative heating was identified as a critical heating source to be understood and an experiment, the Radiative Heating Experiment (RHE), reference K, was identified to help answer the radiation questions. A flight test vehicle was defined, the Aeroassist Flight Experiment (AFE, reference A), to be instrumented to gather, in-flight, the needed data base. The AFE, depicted in figure B, was small aerobrake, STS deployed into low earth orbit (LEO) and rocket driven into the Earth's upper atmosphere at the velocity and entry angle of an ASTV maneuvering from geosynchronous earth orbit (GEO) to LEO. The AFE would perform the aeropass, exit and return to the LEO for STS recovery and return to ground.

The AFE was given new-start approval in 1987. Although cancelled in 1991 due to funding limitations much work was accomplished to solve technical challenges. The Radiative Heating Experiment goals and engineered design were well matured. Many RHE design challenges were successfully met and results of these efforts should have application elsewhere. From the computational standpoint, a specification of the data needed to help validate predictive heating models incorporating radiation transfer was developed. Experiment objectives and flight instrument requirements were developed. The harsh flight environment required development of a window which would withstand the aeropass heating pulse and transmit the needed spectral radiation information to the transducer. Several window concepts were examined and viable designs were tested. The purpose of this paper is to present the RHE experiment objectives and rational, the results of the window development and the expected science return. It is expected that these results will be of interest and use to

designers of other spacecraft mission experiments involving atmospheric entries.

II-FLIGHT MISSION

ASTV FLIGHT PATH

The flight path of a maneuvering ASTV is compared with those of the STS and the Apollo in figure A. The ASTV entry is initially similar to the Apollo entry since both would be returning from relatively distant missions (GEO or lunar). But the ASTV is maneuvered away to decelerate and change its orbital parameters, mainly between 75 and 90 KM, and leaves the atmosphere in an orbit accessible to the STS. Although the STS and Apollo trajectories pass through the ASTV maneuvering altitude, neither substantially alters its velocity there. These vehicles are designed to withstand their major aerodynamic heating at lower altitudes. Their heat shields are overly conservative for their passage through the ASTV altitude and their experience offers little information on which to develop efficient ASTV design codes.

The AFE shape is given in Figure B. It is shaped like an operational ASTVs but at 1/4 scale. It was designed to fly at a constant trim angle of 17° to produce drag and lift and fly a trajectory of an ASTV maneuvering from GEO to LEO. The planned trajectory is shown in Figure F. The atmospheric entry velocity is 9.89 km/sec at 122 km altitude. Navigation control was to be by rolling the spacecraft to redirect the lift/drag vector. The orbit engineers optimized the flight profile around the two indicated velocity/altitude points. The trajectory, from entry to exit would take 600 seconds. Details of the AFE flight are found in Reference M.

III-EXPERIMENT SCIENCE OBJECTIVES

An ASTV would be distinguished from other spacecraft by the incorporation of a large, blunt, aerobrake surface. An ASTV would meet the atmosphere head-on at hypersonic speed and

be exposed to substantial surface heating. This heating would include a radiative component perhaps equal to the convective heating. Accurate predictions of this heating requires the solution of the real gas conditions of the flow field environment of the vehicle. Predictive codes, incorporating realistic gas properties, are being developed at Ames and elsewhere. Predictions of the AFE shock layer properties, from an Ames two temperature aerothermodynamic code, are shown in figure C from reference B. The calculation is for the conditions of peak heating (9.5 km/sec and 77 km altitude). The vehicle size, velocity, and altitude result in a shock predicted to be composed largely of thermally non-equilibrated gas. This is evidenced by the large difference between the high translational temperature, T_t, and the vibrational temperature, T_v, near the shock. This difference diminishes toward the surface to a more nearly equilibrated state. The initial collisions which form the shock convert the kinetic energy of the impact velocity of the air directly into random motion (T_t). Just after the shock T_t is very high, about 50,000 K. Subsequent collisions and other kinetic processes distribute this energy into other internal modes. N_2^+ is formed, N_2 and O_2 dissociate, and reactions proceed to produce NO. The vibrational levels of the molecules eventually are populated and T_v is seen to approach the decreasing T_t. The temperatures relaxes toward each other to about 8500 K as the gas equilibrates. At the low densities of a maneuvering ASTV this relaxation process occupies a significant portion of the shock layer.

An important objective of the AFE was to generate a data base to validate predictive models of radiative heating at the ASTV forebody stagnation region As seen in the figure this heating is predicted to be dominated by emission from the nonequilibrated gases near the shock. The thickness of this region is determined, approximately, by the collisions which drive the gas kinetic processes. For the same maneuver this thickness, and hence the radiative flux from the nonequilibrated regions, is approximately constant with vehicle size (Reference R).. This zone merges with the cooler boundary

layer on small configurations at high altitude conditions (Reference I). This would apply to the size of models which could be used in ground based tests (ballistic ranges, shock tubes, or arc-jet wind tunnels), namely much less than one meter. Validating data from this kind of test would be hampered by a distorted relationship between the kinetic processes as compared with a full scale ASTV. In addition modelling the shock layer of these small shapes would necessitate solving the merged boundary layer also- a different boundary condition from the full scale case. Extrapolation from ground based test results to full scale conditions would involve many uncertainties and require large conservatism. Further, some 3-D calculations have indicated important-processes with relaxation times on the order of the AFE shock layer residence time (Reference H). This phenomena would never be observed on a small test configuration. In contrast, the shock layer of full sized vehicles flying at low altitudes (higher densities) will be mostly equilibrated gases with a very thin, nonequilibrated region at the shock. Apollo and the STS experience most of their heating under this condition. An instrumented subscale ASTV, such as the AFE, flying an ASTV maneuver, was needed to meet the technical requirements. The AFE diameter, limited to the dimensions of the STS cargo bay, was 4.26 meters. This diameter would be adequate to provide a isolating zone of nearly equilibrated gas between the non-equilibrated region of the shock layer and the cooler boundary layer and would provide a suitable platform to develop the data base to help resolve the radiative heating and other ASTV design issues.

SHOCK LAYER RADIATION

The radiating shock region contains a mixture of gases over a large range of conditions and involves many kinetically limited processes (Reference F). The surface flux, even though spectrally resolved, would contains emissions from a complicated source. Surface flux measurements of molecular band systems, for example, would be the aggregate emissions, along lines-of-sight, from the populations of excited molecules over a range of thermodynamic and molecular conditions. Although apparent temperatures (kinetic, rotational and vibrational) would be indicated in the data, they would, in

reality, be the summation of a variety of concentrations and conditions and possibly include absorption. Analysis of this data to understand the conditions within the shock layer would require companion computational models to correlate the measurements with a realistic representation of the physical principles of coupled high speed flight and radiation (spectroscopy). This correlating model would be, of course, an important step toward a validated ATSV design code.

Preliminary codes describing the radiating shock layer of an ASTV have been developed at the ARC. These codes were the basis for developing the science objectives for the RHE. Predictions of the radiant flux onto the surface of the maneuvering AFE were done for species which were expected to be important. Results of these calculations are contained in reference J. Figure E is the calculated spectrum of the radiative flux onto the surface of the AFE near peak heating assuming an optically thin shock (reference B). Molecular systems as well as atomic lines are evident. Atomic nitrogen and oxygen lines are seen in the vacuum ultraviolet, VUV, (100 nm to 180 nm), with the Birge-Hopfield system, (BH-1), of molecular nitrogen as the underlying background. Molecular bands from nitric oxide[4] are seen from 190 nm to 300 nm. Molecular nitrogen[5] systems contribute energy from 280 nm on and then merge with other, stronger molecular bands systems[6] which then dominate the molecular radiation from 300 nm to the infrared. Atomic lines are also seen in the infrared. Very little radiative heating is expected from the infrared beyond one micron.

Because of the subscale size of the AFE, radiative heating is predicted to represent only about 10% of the total heating and is therefore not of overwhelming concern to the AFE. Therefore the RHE was not configured to measure and assess the radiative heating to the AFE, but rather to gather a radiative flux data base to identify the important radiators and

---

[4] NO_γ, $A^2S^+ - X^2P$, and NO_β, ΞΞΞΞΞΞΞ

[5] $N_2(2+)$ bands, XXXXXXXXXXX

[6] $N_2^+(1-)$, $B^2S_u^+ - X^2S_g^+$, CN_V, $B^2S - X^2S$, and $N_2(1+)$, $B^3\Sigma_g - X^3\Sigma_u^+$

to validate the calculated gas properties of the flow field calculations including radiative transport. Such a validated model could then be used to establish the requirements for an efficient full scale ASTV heat protection system.

Vacuum Ultraviolet:

Some of the atomic lines in the VUV are extremely intense and are the subject of concern. Various models of these line emissions predict widely different radiative heating levels ranging from insignificant amounts to levels dominating the overall heating (references B, C, and D). Since the VUV emissions are from transitions to the ground states a description of the surface flux is complicated by spectral absorption from a range of condition of the absorbers between the emitters and the surface. A realistic, predictive model must include accurate details of the absorption and emission. Calculations at the ARC (reference B) indicate that if the VUV line radiation would reach the surface unabsorbed, the resulting heating would be vastly more than the convective heating. The VUV emission is from the nonequilibrated regions close to the shock. Here the spectral lines are strongly doppler broadened by the high kinetic temperature. The cooler parts of the shock and boundary layer are calculated to absorb these strong features directed toward the surface. But these cooler absorption regions have spectrally narrower absorption features resulting in the curious effect that the intense region at the line center is absorbed and only the energy in the wings reaches the surface with any heating significance. The total line emission can be calculated reasonably precisely. But the problem of the overall absorption is difficult because accurate spectral distributions of energy over the emission line shape, and over the absorbing line shape are needed to properly determine the ultimate energy reaching the surface. The Ames model predicts that absorption will reduce the VUV flux by 99.8% to represent about 25% of the radiative heating of the AFE, but errors in the calculated line shapes could result in disproportionate errors in the prediction of surface heating rates.

ARC predictions (reference B) of the total flux from all of the VUV atomic lines over the AFE trajectory are plotted in figure J together with predictions of the total radiative surface flux and the flux from the group of 174 nm atomic nitrogen lines. The predictions are not accurate at the low densities where the intensities are low ($0<t<60$ seconds, and $t>250$ seconds) and are represented herein only as qualitative. The total radiation from the VUV lines is predicted to be controlled by self absorption, and become optically thick, throughout the period of significant radiant heating. The importance, and perhaps spectral details, of the heating from these intense VUV lines needs to be ascertained. The lines at 174 nm contribute substantially to the total VUV and they too become optically thick. Of primary importance is to obtain measurements of these lines during the initial portion of the aeropass, while the radiation is at low optical density, the increase to optically thick conditions, and adequately into the subsequent optically thick region to establish its intensity. Also important, but secondarily, would be the analogous measurements on the outward leg of the trajectory to establish the transition from optically thick conditions to as far as the intensity would permit. These measurement periods are seen from figure J to be from entry to 100 seconds, and from 200 seconds to exit

UV-Visible:

Most of the heating of a maneuvering ASTV is predicted to come from the strong $N_2^+(1-)$ and CN_v molecular band systems in the near UV and visible regions of the spectrum. From the viewpoint of heating this spectral region is probably optically thin. Measurements of the detailed spectral radiative flux in this region would help identify unexpected, but important, radiators in the shock layer, and would be the basis to validate predictions of the conditions of the importantly radiating gases. Code validation of these measured molecular spectral features would be a very powerful validation of the predictive capabilities.

Infrared:

Rich and diagnostically important atomic line radiation is predicted from oxygen and nitrogen in the infrared. These

lines also emanate from the hot regions near the shock. The range of intensities of these lines is from weak (unabsorbed) to moderate (partially absorbed) levels. Measurements of the unabsorbed lines would yield information, unmodified by absorption, about the emission phenomena which is from the gas near the shock. Measurements of the flux from the partially absorbed lines would yield information about the absorption properties of the intermediate, cooler gases

Under the conditions of a maneuvering ASTV electronic excitation of these atoms is by electron collisions. Measurements of the IR line intensities would help validate predictions of ionization levels and electron gas temperatures. The absolute measurements of the intensities of these lines could also help determine the atomic density profiles through the shock.

IV-RHE INSTRUMENT PERFORMANCE

The objective of the AFE was gather flight data to help develop the design technologies needed for efficient ASTVs, and the RHE objective was to provide data to address the radiation issues. Since the radiating medium was complex in composition and state, surface flux measurements alone would not be useful. The RHE relied on companion predictive codes to develop the objectives, and would also rely, in turn, on these codes for post flight data interpretation. This experiment/code relationship concept was successfully employed in a pioneering flight experiment, the PAET (Reference L). PAET was an Earth entry experiment which measured shock layer radiation with none spectrally resolved radiometers. The data was combined with results from a computational model to determine properties of the ambient gas. This test was designed to demonstrate the potential to obtain data during the high speed entry of a planetary probe which could be used to determine the atmospheric composition.

Successful predictions of the observed RHE quantities by the physics of the gas chemistry and spectroscopy incorporated in

the computational codes would require matching of many observed quantities. Consistency of the results would in turn result in confidence in the predictions of the details of shock layer gas conditions. The RHE was to make absolute spectral measurements of the stagnation region surface flux, under conditions of important radiative ASTV heating, to validate the VUV and longer wavelength radiation calculations, and to help determine the shock layer gas conditions (concentrations, Tk, Tv, Tr and Te).

In each case measurements would be made at several locations through windowed penetrations of the AFE stagnation region heat shield.

These objectives, with predictions of the surface radiative flux, (see figures C, J and E) formed the basis for the RHE instrument performance requirements. The requirements were, in part, as follow below:

Obtain spectrally resolved surface flux data from the AFE stagnation region gas cap. Measure the flux from the atomic nitrogen lines at 174 nm to provide assessment of the VUV calculations. Measure the range from 200 nm to 900 nm with sufficient spectral resolution for code validation;

Obtain spectrally integrated data using a wide band detector, such as a blackened thermopile, to measure the spectral radiation from the VUV to the IR. This data would provide a level of redundancy with the spectral instrument, and would help determine the sufficiency of the spectral data to provide validation for overall radiative heating;

Provide a windowed aperture to isolate the detector from the shock layer gases. The window to be mounted flush with the spacecraft surface so as to not disturb the boundary layer flow; and

Obtain a broad band measurement and a complete spectrum every 3 seconds during the 600 second AFE trajectory.

These requirements formed the basis for a Request for Proposal and a fully competed contract was awarded to Martin Marrietta Corporation, Denver, CO.

V- RHE INSTRUMENTS

The contractor developed the design of the instruments and completed a CDR for all but the windowed aperture. The final design is summarized as follows.

The contractor determined that instrument requirements could be met using a small, grating spectrograph (0.125 meter focal length) with a scanning, linear photocathode array detector. The UV spectral sensitivity of a sample, windowless, commercially available, array detector was measured to extend to below 160 nm by the contractor team (reference N) . Their measurement result is shown in Figure H. Spectral resolution of 0.6 nm from 174 nm to 800 nm was thereby attainable. Their sensitivity measurements, together with predictions of the radiation intensities, showed that this setup was adequate to meet the scientific objectives including intensity measurements of the 174 nm atomic nitrogen lines.

Sensitivity and dynamic range requirements for the spectrally integrated data were met with a thermopile detector. The spectral response of such a detector, for purposes herein, would only be limited by the window transmission.

FLIGHT WINDOW DESIGN

The window design was not matured to a CDR level at the time of program termination. Although a flight article had not been designed and tested, considerable progress had been made. Viable designs, which would survive the aeropass and meet all or part of the experiment objectives, had been developed and tested. The results indicated window configurations which have a high likelihood of flight worthiness. This section describes these designs and their expected science return.

Requirements:

Window design requirements included adequate optical performance to meet the scientific objectives and survivability to not compromise mission safety. The scientific objectives required, in part, that the window transmit radiation over the range of interest, e.g., from 174 nm to several microns, over important portions of the trajectory. The widow and its mounting would experience high convective heating rates which might include heat liberated from catalytic reaction of recombining atoms diffusing to the surface, and thermal shocks.

Sapphire was determined to be the material of choice for the window (Reference O).

Spectral transmission:
Sapphire, at room temperature, transmits ultraviolet radiation from well below 174 nm to well into the IR. The short wavelength cutoff of sapphire's transmission is due to the long wavelength edge of a broad absorption band. At elevated temperatures this band widens. Thus the shortest VUV wavelength transmitted increases with temperature. A discussion of this phenomenon, from the standpoint of glasses, is in Reference Q. The maximum sapphire window temperature which would be useful for measurements at 174 nm was measured by us (Reference O) to be about 800 C (1472 F). This was done by measuring the 174 nm transmission of a heated specimen window. The measurement results are shown in Figure L.

The short wavelength cutoff of sapphire infrared transmission, about 5 microns, insures that the aeropass heating will not degrade the optical transmission at the IR wavelengths of interest herein (e.g., 1 micron).

Window heating:
The AFE aeropass heating rate is shown in figure D. This heating pulse would rapidly raise an uncooled window to temperatures well above 800 C. Indeed, during simulated aeropass heating testing in an arc-jet wind tunnel, uncooled sapphire reached its melting temperature (2040 C) and

ablation was observed. Because of sapphire's low infrared emissively radiative cooling does not significantly help maintain the desired temperature. The minimum design requirement, which could meet the science objectives, is that the window maximum temperature not exceed 800 C for at least the first 100 seconds of the entry, and then if possible during the period after 200 seconds with a desired goal of maintaining the temperature below 800 C for the entire aeropass.

To achieve the required ultraviolet performance the entry heating would have to be offset by a thermal mass to maintain a manageable temperature.

Window designs:

A development program was conducted and several designs concepts were built and subjected to laboratory tests. These tests consisted of exposing the windows and their mounting configurations to various heating loads simulating the AFE entry heating and included aggressive, overly conservative, testing in an arc-jet wind tunnel (reference O). Successfully surviving these tests would insure that the design would survive the aeropass and not pose a risk to spacecraft or the experiment. Some of the tests specimens were instrumented with thermocouples to develop computational models of the in-depth thermal response of the window and its mount during the arc-jet tests (reference P). These models were in turn used to predict the thermal response during the flight mission.

Two design, one uncooled and one cooled, were shown to be promising as bases for design of a flight window which would survive the AFE entry environment and yield scientific data. Both designs used niobium in the construction of the mounting hardware. The regions of the niobium which could be exposed to the shock heated air were coated with a silicide coating to protect them from chemical erosion (reference P).

A design, called the uncooled design, employing thermal isolation between the sapphire and the mount was configured. Alumina paper and fibrous insulation (FRCI-15, STS type heat

shield material) was used to reduce the thermal conductance between the sapphire and its mount as shown sketched in Figure O. This design was instrumented and tested in the arc-jet wind tunnel Windows of 13.7 mm diameter and of thicknesses from 1 mm to 3 mm were not damaged during the arc-jet tests.

Predictions of the thermal performance of the uncooled design during the AFE aeropass are shown in figure M. This window would be adequate to gather data UV-VIS and IR spectral regions over the entire trajectory. However the hottest portion of the window is predicted to reach 800 C at about 130 seconds into the trajectory. This would allow measurements of the 174 nm region for the initial portion of the trajectory but would be too hot during the period after 200 seconds.

Two cooled designs were evolved by the contractor. Both windows were cooled by conduction through a copper element to the metallic mounting and thence to a heat sink. High thermal conductivity was assured by a copper element which was brazed with a eutectic bond (developed by Martin Marrietta Aerospace Group) to the inner surface of the sapphire and in turn was brazed to the upper end of the support tube (reference O). One configuration employed a 14.5 mm diameter window with a copper screen, 50% open, bonded to the surface as the copper element. A smaller window configuration was 10.7 mm diameter and a copper washer bonded to the flat edge of the window. Both of these configurations were built and were not damaged during the arc-jet tests. Both designs would transmit the same amount of radiation and would satisfy aperture requirements of the experiment.

These cooled configurations are shown sketched in Figure K.

Predictions of the performance of the cooled designs in the configuration of the test specimens were not made. Instead a recommended cooled design was developed based on these test results. This design is shown sketched in figure P Note that this design shields the silicide coated areas of the holder by

overlapping the heat shield material. This would reduce the problem of possible window contamination from the coating. This problem is discussed below under "Window Contamination". Predictions of the thermal performance of this design during the AFE aeropass are shown in Figure N. The maximum temperature of this window remains below 800 C for the entire aeropass so this window would meet the thermal goal. The scientific objectives could be met over the entire aeropass.

SOLAR CALIBRATIONS

In order that the RHE data be useful, it must be credible. Experience with absolute measurements of radiation teaches the value of calibrating before and after a measurement. But the RHE instrumentation would not be available for laboratory testing for a substantial period before the flight, perhaps as long as one year, and for a substantial period after the flight. The sun would provide a useful calibration source which would be available just before and just after the aeropass. The source strength can be well characterized and there is no problem with atmospheric interference. The UV-Vis to IR spectral region would be well calibrated but scattered light problems within the spectrograph would make calibration at 174 nm difficult. A spectrally selective filter would probably be required during this calibration.

Calibrations using the sun were deemed to be important to insure credibility of the data. However these calibrations required spacecraft resources to be expended to point each radiometer in turn at the sun. In addition the radiometer view field needed be adequate to accommodate errors in navigation, pointing accuracy, and spacecraft drift during the calibration time. In the AFE case a circular, radiometer view field of 22 millisteradians was be required to guarantee capture of the entire sun's disc without vignetting. The radiometer mounting requirements behind the heat shield dictated a window diameter of 14.7 mm to achieve this viewfield. The arc-jet tests suggested that an uncooled window this size would suffice at the cost of the later period VUV data. The larger cooled window required a screen brazed over the entire under surface

of the sapphire, the presence of which would make it difficult or impossible, to guarantee what fraction of the sun was obscured by the opaque portion of the screen.

Window lens:

The maximum window diameter (based on performance requirements) with the minimum distance from the window to the instrument aperture (based on spacecraft requirements) will not subtend an adequate viewfield for solar calibrations needs. The view field of the small, edge cooled window could be increased to without compromising the radiometer objectives by fashioning the inner surface of the sapphire into a negative lens. The effect would be to increase to viewfield of the for solar calibration purposes without decreasing the sensitivity with respect to the shock layer radiation from that of the flat cooled windows. With respect to the radiometer the radiating shock layer is an relatively uniform, extended source but the sun is a discrete source. Such a lens will slightly alter the region of the shock being measured but would not change the shock layer flux reaching the radiometer. An illustrative design, based on the dimensional requirements for the AFE, of a lens-apertured window is shown in Figure Q. A virtual image of the solar disk is formed within the extended field of view of the internal solid angle. The negative curvature required is very small and would have negligible effects on lessons learned during the arc-jet tests. Use of data gathered under this configuration would, of course, require a different geometrical interpretation of the radiating regions of the shock layer contributing to the signal.

WINDOW CONTAMINATION:

Window contamination is a serious concern to the credibility of the data. Trace window contaminates can significantly increase the uncertainty of radiometric data, particularly if the ultraviolet. Sensor windows can be fouled during all phases of the AFE mission by contaminants form a variety of sources. Any spacecraft experiment expecting to gather reliable radiometric data will have to be particularly critical of the presence and thoroughness of a contamination control activity to identify, assess, and control the problem. An estimate of the

expected contamination, from an inventory of known contaminants, is important to help assess the validity of the solar calibrations and the data. Three types of window contamination, their sources, and implications for this kind of mission application are discussed below.

Particulates (i.e., dust)
Sources include dust-laden air after the "last access" point when no further cleaning or inspection is permitted, launch vehicle (i.e., STS or other carrier) payload bay dust dislodged during launch, orbit operations in the vicinity of the launch vehicle, and particulates ejected by maneuvering rockets, RCS, from either the launch vehicle or the spacecraft.

Protective covers should protect the windows during most ground operations. After final cover removal and cleaning, a characterized clean room environment should be maintained. Vertically positioned radiometer windows will reduce agglomerate of particulates to about 5% of the horizontal rate in a one G environment. The mission activity is different. During the launch of the STS, for example, payload bay dust, including dust from companion payloads, is violently agitated and then "settles" uniformly of all exposed surfaces.

The particulates from the RCS activities can be ameliorated simply by avoiding the spray pattern of the RCS engine. Monopropellant grade hydrazine can contain as much as 1 mg/liter of particulates and a high purity grade is available if required.

The effect of contamination from these particulates should be fairly non-wavelength sensitive and an assessment would be possible from the solar calibrations.

Volatile contaminates (compounds of small molar mass, e.g., H_2O or NH_3):
These contaminates are threats to optical surfaces if they chemically attack the material, or if they are deposited as aerosols containing dissolved solutes that are left behind after evaporation. Potential sources are migration from saturated

surfaces, and from thruster motors venting and exhaust products. Air-borne aerosols, particularly of NaCl in water, could be a problem, for example, at Kennedy Spacecraft Center due to its proximity to the ocean.

Nonvolatile contaminates (nonvolatiles of large molecular mass such as polymeric compounds, including silicone derivatives.: This class of contaminant is the most deleterious to the radiometry experiments. They can be derived from a variety of sources. They are difficult to remove and in general are strong radiation absorbers, particularly of UV photons. Sources of these contaminants are the spacecraft itself, the payload bay, and companion payloads. The are generated primarily from polymeric compounds, i.e., plastics that are used as matrix binders, in circuit boards, films, adhesives, or coatings. With respect to the AFE silicones were very worrisome in this regard because they are used extensively in the heat shield bonding and they will probably bond strongly to the window material. Solar heating of the spacecraft, and the resulting increase of production of these contaminants, in the vacuum before atmospheric entry, poses a special situation to be assessed. The firing of a major rocket motor can also be a source of nonvolatile fouling as well as the thermal degradation of the polymeric insulation liner after shutdown. During the aeropass contaminants generated from the heat shield by the atmospheric heating will be carried in the boundary layer flow and possible deposit on the windows. In order to quantify the sensitivity to this form of contaminant as estimate was made of the allowable level of film thickness of nonvolatile contaminants. To limit beam attenuation to less than 1.5% at 200 nm, the maximum allowable film thickness is 0.5 nm assuming the reasonable value for the extinction coefficient of 0.0002 nm^{-1}. Considering the probably molecular size of these compounds this value undoubtedly represents a less than monomolecular layer.

Silicide coating contamination:
As seen in figures O and K, the designs of the arc-jet wind tunnel test specimens included a silicide coating on the metallic portions of the window mount which would be exposed to the

flow. Spacecraft experience has shown that this coating is effective in eliminating the metal erosion during atmospheric entries. This coating could likely be part of the design of the flight windows. It was therefore of interest to address possible material from this coating contaminating its adjacent window. The environment of the arc-jet free stream contains contaminants from the arc heater so examination of the window was not conclusive. Several tests were conducted to compare emission spectra from the radiating region near the window with and without a silicide coated holder. Material ejected from the silicide, entering the boundary layer, should show added spectral features. The setup is shown in Figure R. Spectra were taken from XX nm to XXnm and no differences were noted. This test was encouraging but not exhaustive enough to validate flight design performance. Further work would be required if this material were to be used.

The high importance of controlling contaminants requires that a high priority be given to this at every phase of the experiment, spacecraft and mission design.

VI- CONCLUSIONS

Experiment objectives for the Radiative Heating Experiment of the Aeroassist Flight Experiment are described. Although the project was cancelled, the design of the experiment were well matured. The instruments, with the exception of the windowed aperture, had successfully completed a Contractors Design Review. The experiment goal was to develop a data base characterizing the radiation flux incident on the stagnation region surface of an aerobrake returning from GEO mission. The purpose of the data base was to refine and validate aerothermodynamic computational models for these vehicles. The experiment objectives, based on this goal, was to obtain stagnation region surface flux, with 0.6 nm spectral resolution, from 174 nm to 900 nm, during the aeropass. There are serious questions about the importance of the VUV radiation from atomic lines. To help answer this concern data from the atomic nitrogen at 174 nm is shown to be required from entry until about 100 seconds into the trajectory and from about 200 seconds on. Instrument

performance specifications were generated from these requirements were a small grating spectrograph using a UV sensitive linear array was found to meet the specifications. Special, windowless arrays, were found to be useful at 174 nm.

Although the window had not reached the maturity of the instruments, considerable progress had been made. The entry environment of high heating and exposure to the shock layer plasma present special problems. Sapphire was chosen as the material of choice. Window temperatures needed to be below 800 C for use at 174 nm. Small sapphire windows, both cooled and uncooled were built. The former were conductivity cooled through a copper screen or washer brazed to the sapphire. The latter were insolated by ceramic material from the heat sink. Both of these kinds of windows successfully withstood overly conservative arc-jet wind tunnel testing. Scientific performance predictions of these windows were made based on theoretical models of the radiant flux during the entry, and on window thermal performance models based on instrumented arc-jet tested specimens. Three designs are described which would partially or totally meet experiment objectives and would form the basis for the design of a flight window. A recommended design is described.

The importance of credibility of the data is discussed in the context of absolute calibrations and window contamination. Solar calibrations were designed as part of the mission scenario. The influence of these calibrations on window requirements is discussed and the use of a lens instead of a flat window is shown to be possibly required. Window contamination is important and requires special consideration by the experiment and mission designers.

References

Reference A

Williams, L., Putnam, T., Morris, R., "Aeroassist Flight Experiment", Aeronautics Division, Headquarters, National Aeronautics and Space Administration, Washington, D.C.

Reference B

Whiting, Ellis E., and Park, Chul, " Radiative Heating at the Stagnation Point of the AFE Vehicle", NASA TM 102829, November 1990.

Reference C

Carlson, L. A., "Approximation for Hypervelocity, Non-equilibrium, Radiating, Reacting, and Conducting Stagnation Regions", AIAA Thermophysics, Plasmadynamics and Laser Conference, June 27-29, 1988, San Antonio, TX, AIAA Paper 88-2672.

Reference D

Moss, J. N., "Non-equilibrium Thermal Radiation for an Aeroassist Flight Experiment Vehicle", AIAA Paper 88-0081, Jan. 11-14,1988.

Reference E

Palumbo, G., "Shock Layer Vacuum UV Spectroscopy in an Arc-Jet Wind Tunnel" NASA TM 02258, January, 1990.

Reference F

Park, C., "Problems of Rate Chemistry in the Flight Regimes of Aeroassisted Orbital Transfer Vehicles", Reprinted from "Thermal Design of Aeroassisted Orbital Transfer Vehicles", H. F. Nelson ed., Progress of Astronautics and Aeronautics, 96, 1985.

Reference G

Palumbo, Giuseppe , Craig, Roger and Carrasco, Armando., "Spectral Measurements of Shock Layer Radiation in an Arc-Jet Wind Tunnel"

Reference H

Reference which showed the AFE radiation peaking along the surface (Chandler)

Reference I

For the same manuveur this thickness, and hence radiative heating from the nonequilibrated regions, is approximately constant with vehicle size. In the cases of small, ground based test shapes, tested at high altitude conditions, this zone merges with the cooler boundary layer (reference I).

Reference J

Whiting and Craig "Handbook of AFE Stagnation Region Radiant Flux Calculations"

Reference K

Davy, W .C., Park, C., Arnold, J. O., and Balakrishnam, A., "A Radiometer Experiment for the Aeroassist Flight Experiment", AIAA Paper 85-0967, June 1985.

Reference L

PAET

Reference M

Data Book Documentation: AFE Aerobrake Aerothermodynamic Data Book for Baseline V Trajectory, prepared by the Lockheed Engineering and Sciences Company under contract NAS 9-17900 for the Aerosciences Branch, Advanced Programs Office, Lyndon B. Johnson Space Center NASA, Houston Texas, JSC-23623, April 1989.

Reference N

Private communication: Laura Wood and XXX for measurements of the VUV response of the array.

Reference O

Terrazas-Salinas, Imelda, "Development of Radiometer Windows for Atmospheric Entry Vehicles", Paper 93-142, Proceedings of the 39th International Instrumentation Symposium, pps 1031 to 1049, Albuquerque, New Mexico, May 2-6, 1993

Reference P
Private communication: A. Stewart and Thomas Squire to James O. Arnold, RTM:234-1, 9/92.

Reference P
Private communication: Silicide coating for niobium

Reference Q
Wedding, Brent, "Measurement of High-Temperature Absorption Coefficients of Glasses", J of the American Ceramic Society, 58, no 3-4, pages 102 to105, Mar-Apr, 1975

Reference R
Binary scaling rule

Figures

Figure A. Flight path of a maneuvering ASTV is compared with those of the STS and the Apollo

Figure B. The AFE shape

Figure C Calculated stagnation region properties, from reference B)

Figure D Calculated aeropass heating rates for the AFE

Figure E, Prediction of the important surface heating radiation flux onto the surface of the AFE from reference B.

Figure F Predicted flight of the AFE spacecraft. Show pylons.

Figure G Artists depiction of an ASTV maneuvering through the Earth's upper atmosphere

Figure H Measured MM uv response of the linear detector.

Figure J Prediction of the surface intensity of the 174 nm atomic nitrogen lines, all VUV lines, compared with the overall radiative surface flux over the AFE trajectory. The regions important to acheive the VUV data are indicated.

Figure K
Test specimens of cooled Sapphire radiometer window designs. One utilized a XXXmm diameter window brazed to a perforated copper heat transmission plate, and the other utilized a XXXXXmm diameter lens edge cooled.

Figure L
Sapphire transmission as a function of temperature.

Figure M

Temperature history of uncooled window during the entry.

Figure N

Temperature history of cooled window during the entry.

Figure O

Sketch of thermally isolated sapphire window assembly

Figure P
Sketch of recommended cooled RHE window design. The window holder is shielded from the shock region gases by overlapping the coating.

Figure Q
Sketch of lens aperture.

Figure R
Sketch of setup to mearsure radiation from material removed from the silicide coating.

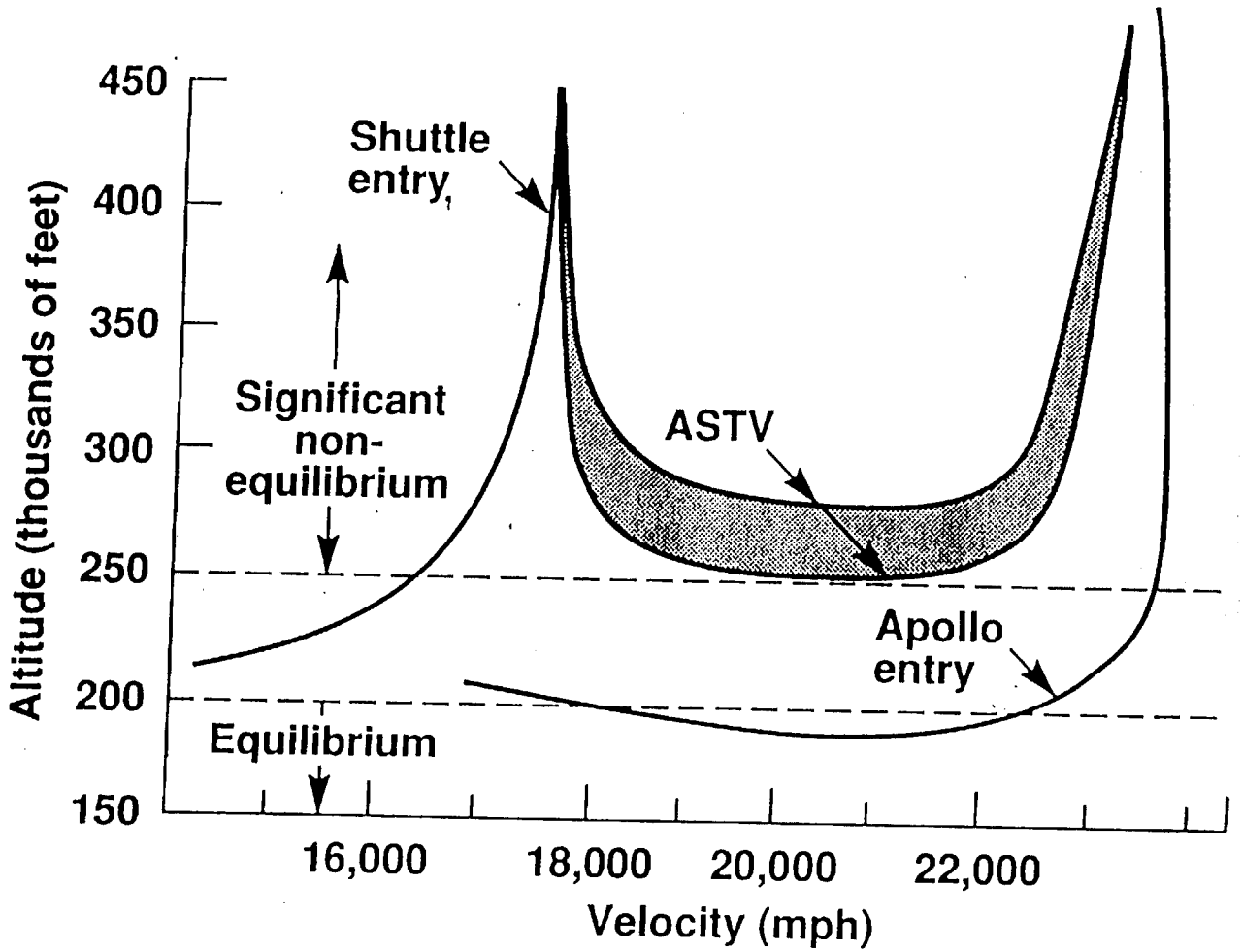

FIGURE A

ASTV FLIGHT REGIME COMPARED WITH STS AND APOLLO

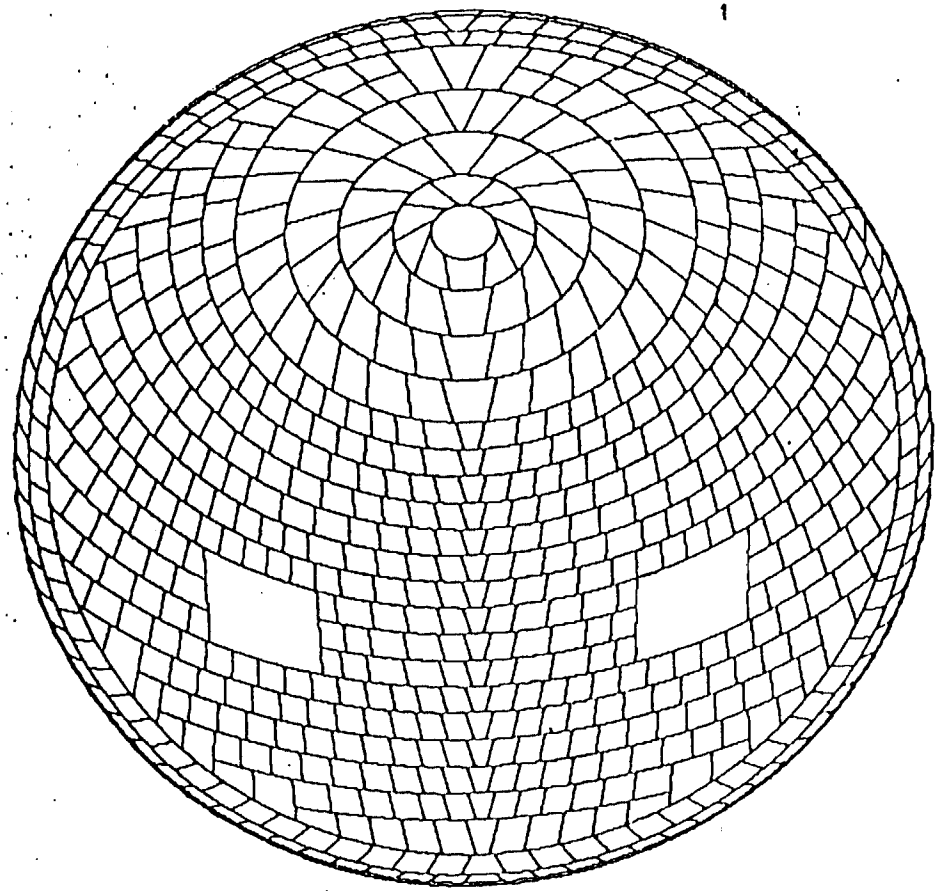

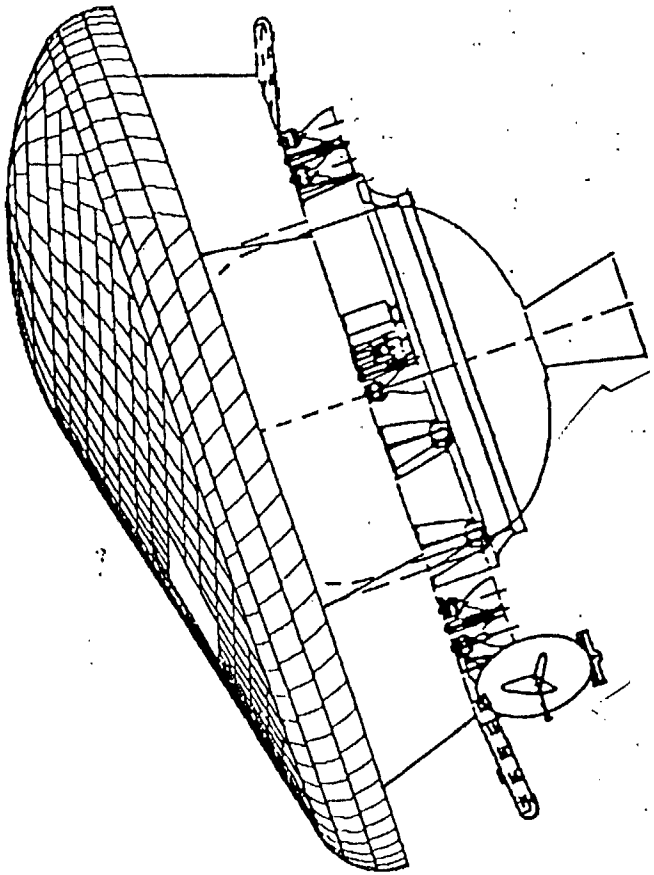

FIG B

AEROASSIST FLIGHT EXPERIMENT
SPACECRAFT SHAPE

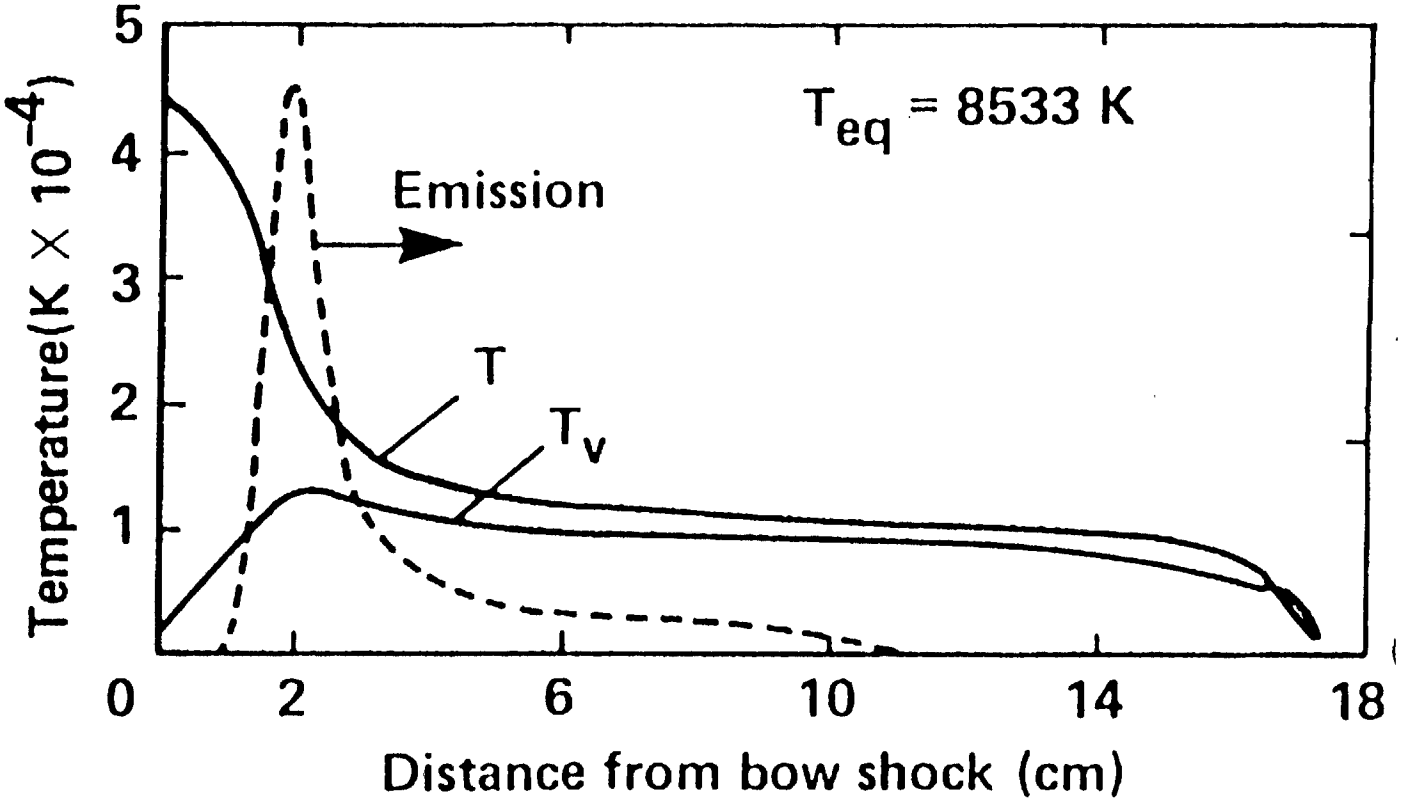
5
4
3
2
1
0
2
6
10
14
18
Temperature(K × 10⁻⁴)
Distance from bow shock (cm)
T_eq = 8533 K
Emission
T
T_v

FIGURE C

JSC 23571
5/89

Fig D

AFE Aeropass Heating Rates

Baseline V

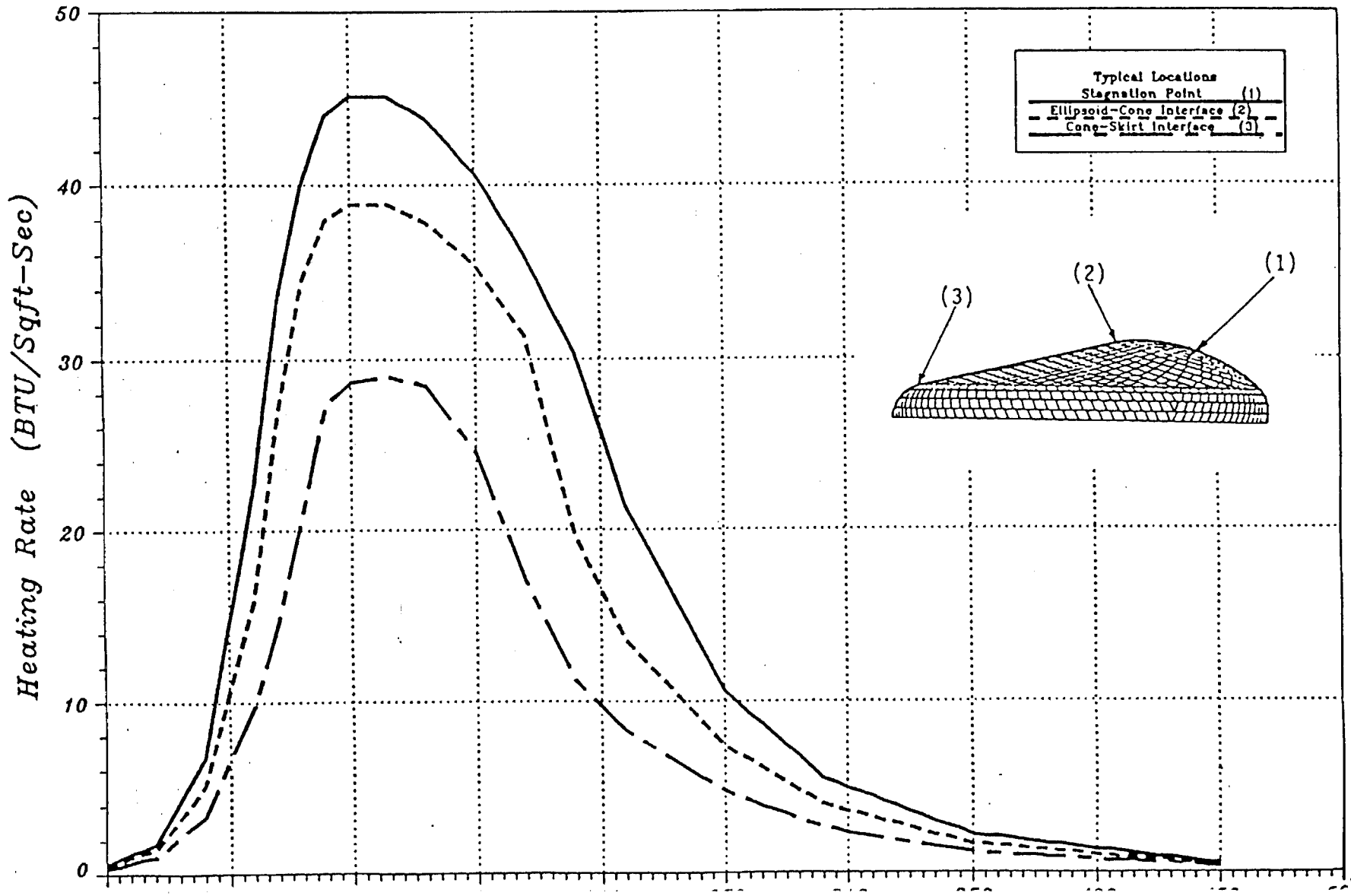

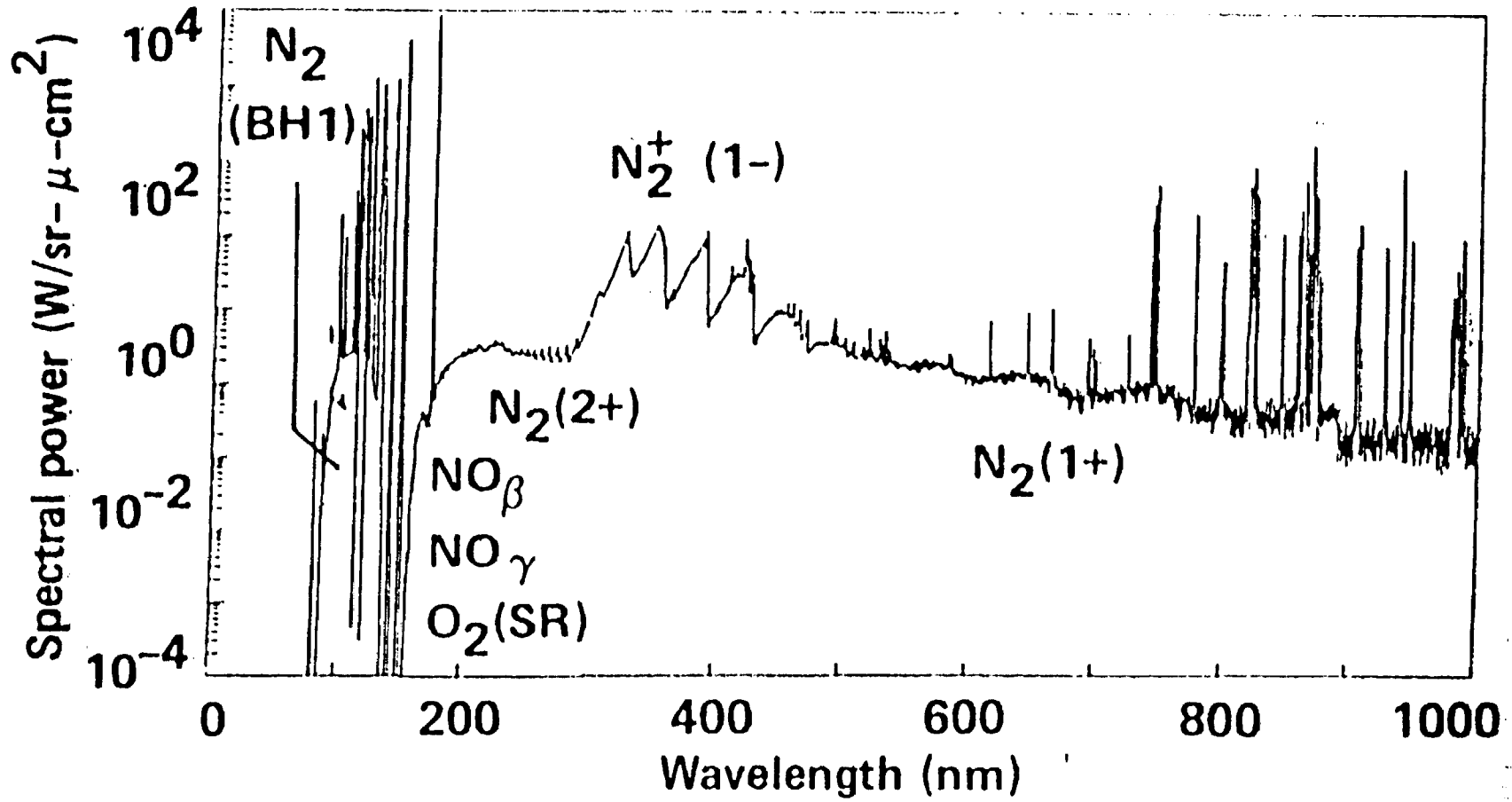
Spectral power (W/sr-μ-cm²)
10⁴
10²
10⁰
10⁻²
10⁻⁴
N₂ (BH1)
N₂⁺ (1-)
N₂(2+)
NOβ
NOγ
O₂(SR)
N₂(1+)
0
200
400
600
800
1000
Wavelength (nm)

FIGURE E

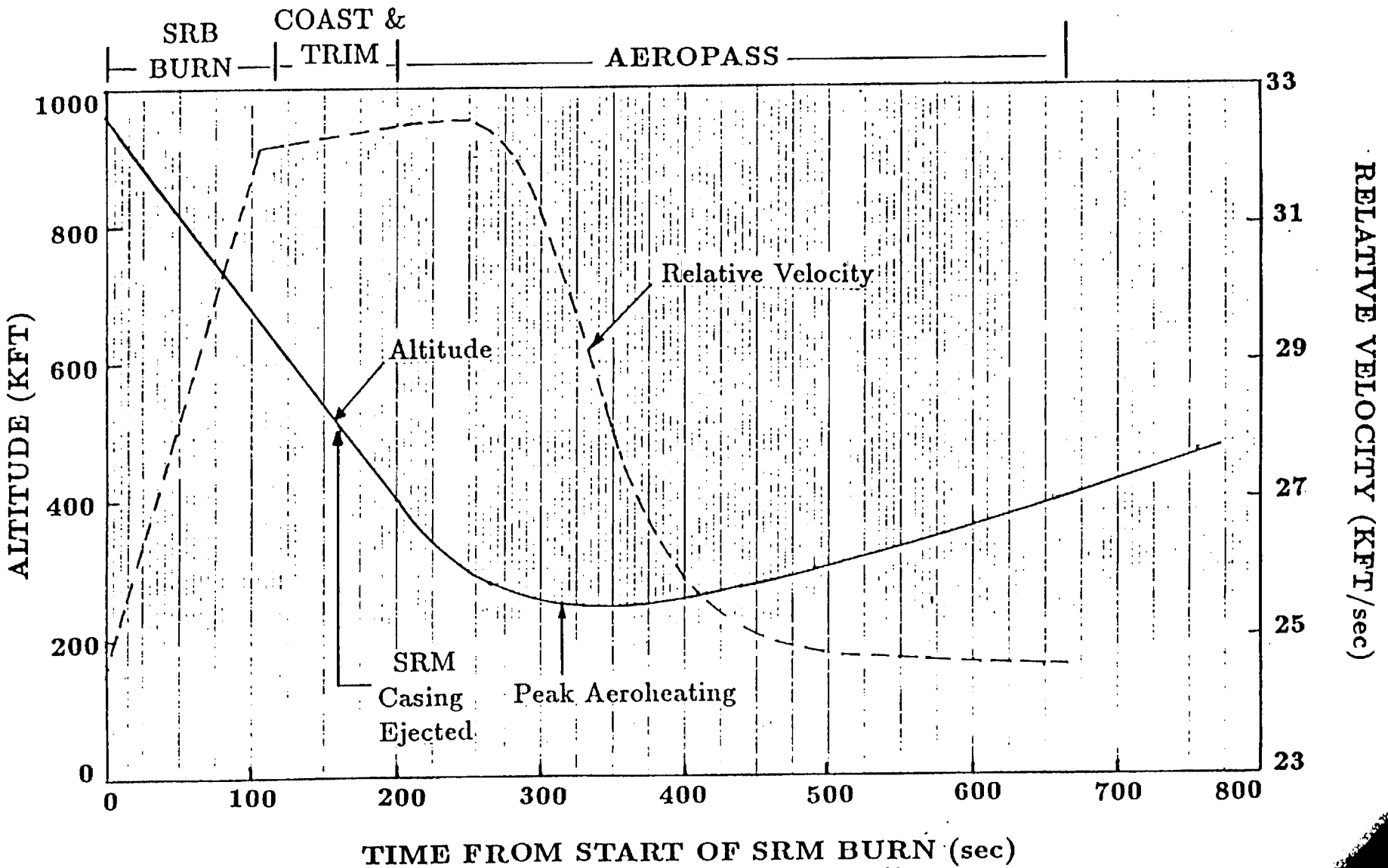

Figure 3.1: AFE Trajectory During STAR 63FD SRM Burn and Aeropass for a 4100 lb. Vehicle. The Aeropass Trajectory is the Baseline 5, 3-sigma Trajectory.

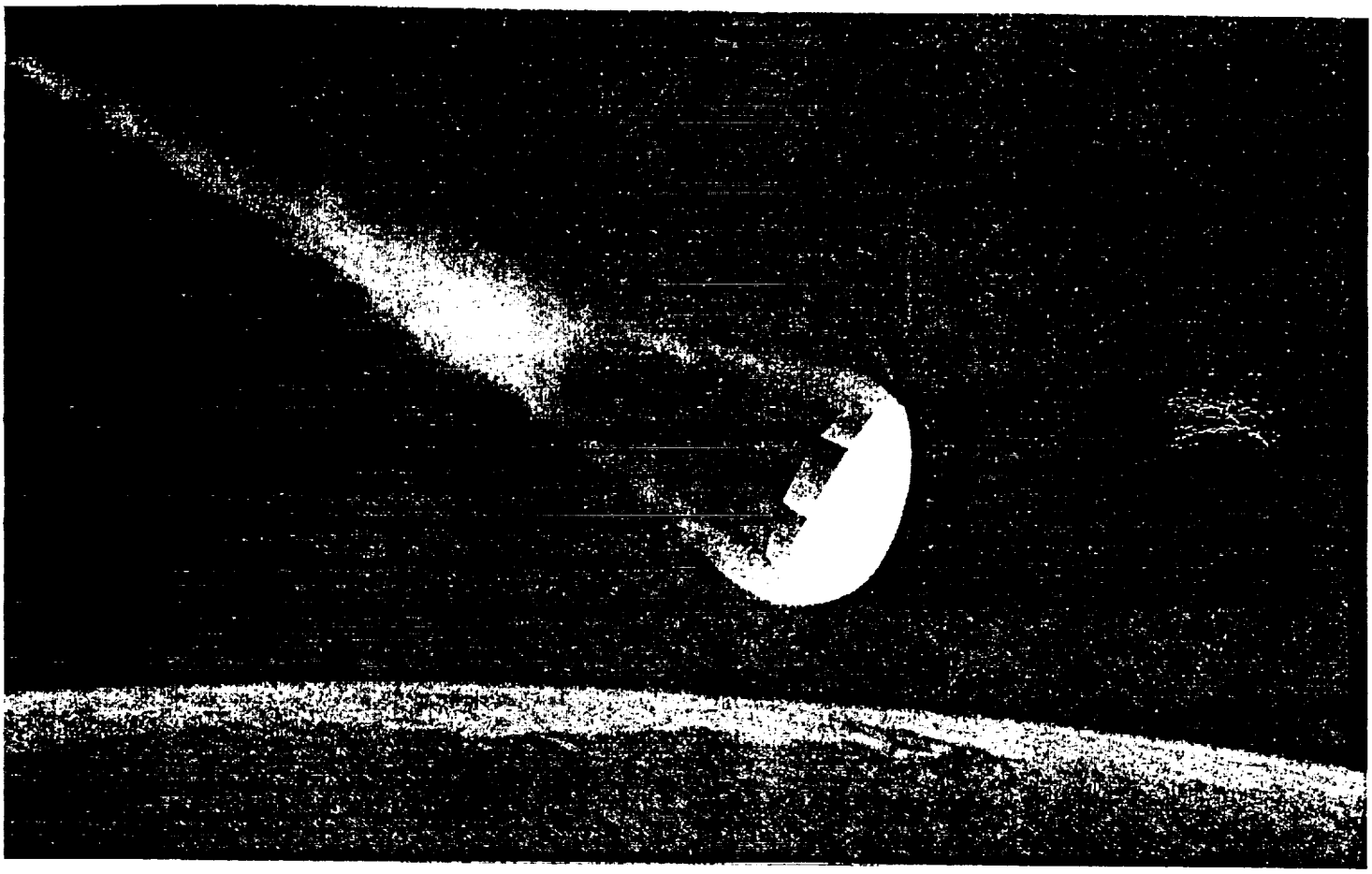

FIG 6

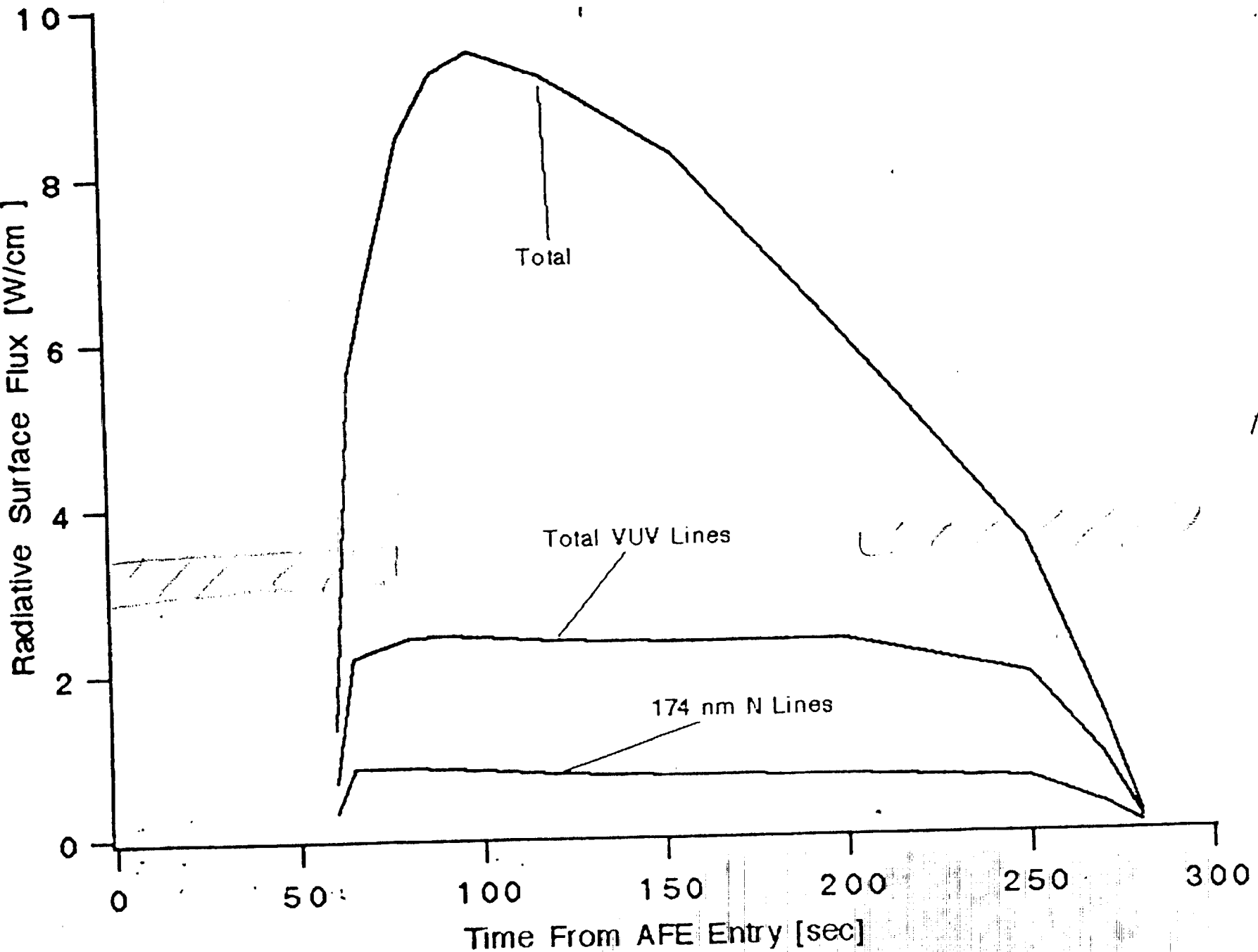

Figure 3

Windowless Array

NORMALIZED RETICON RESPONSE (PMT STD)

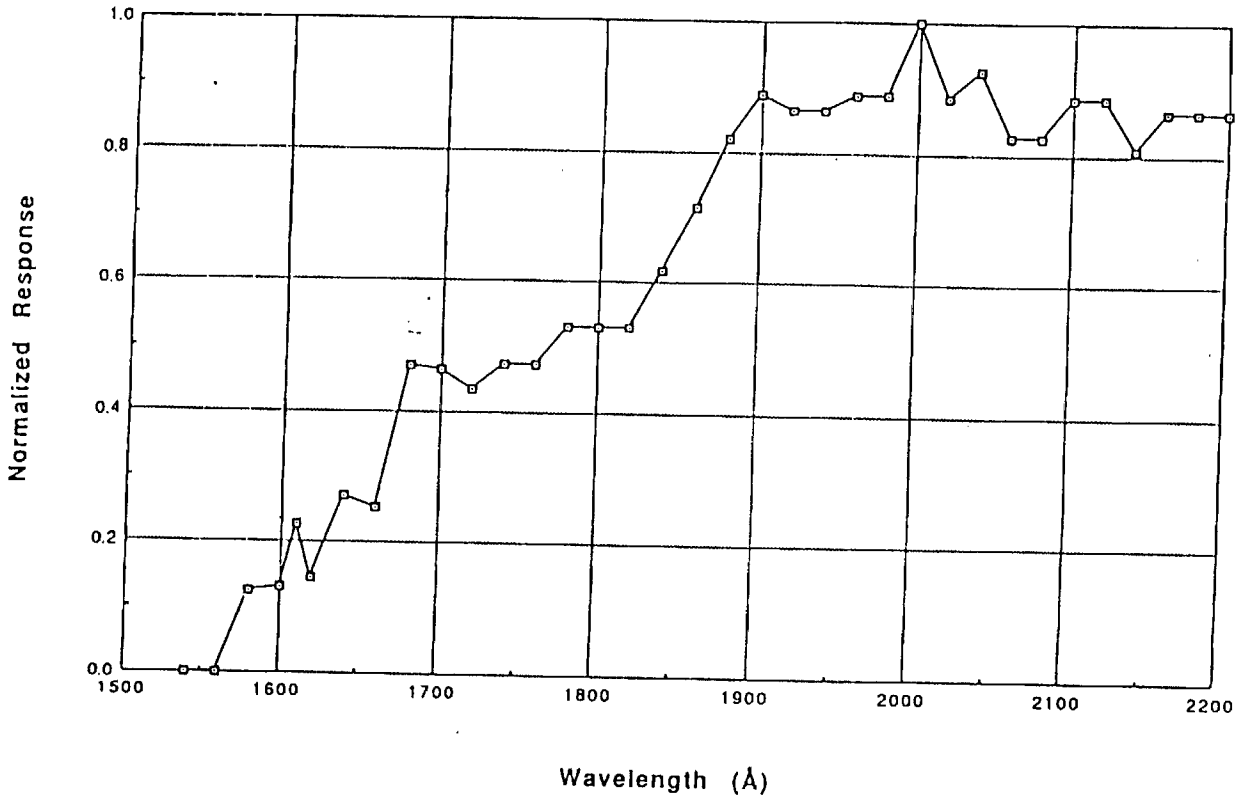

Figure 4

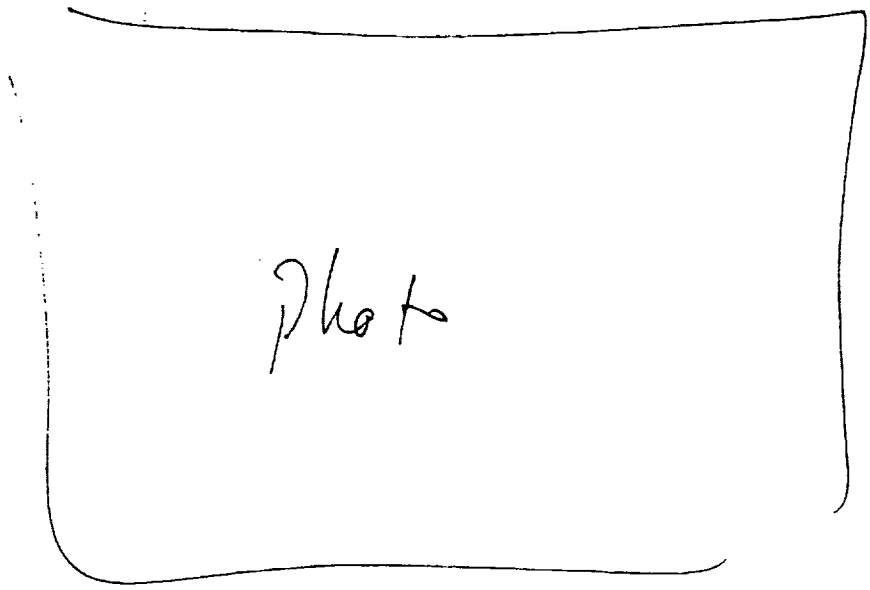

Fig K

Test specimen of coiled windings

FIG 1

Sapphire T vs Temp

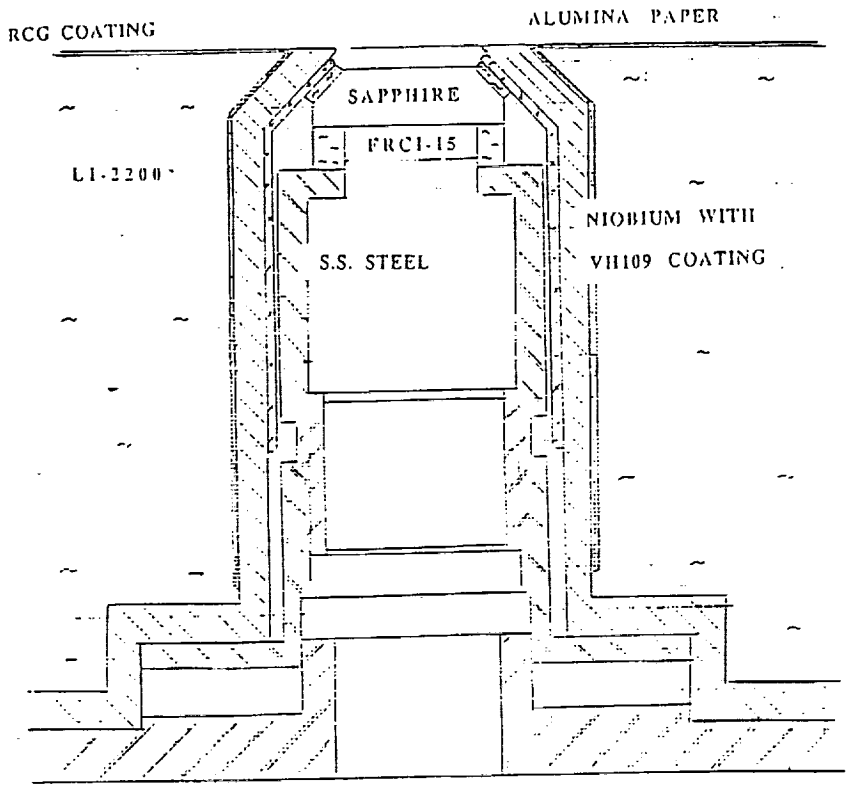

needs leaders to clarify materials

Figure O

Sketch of test article for the themally isolated sapphire window.

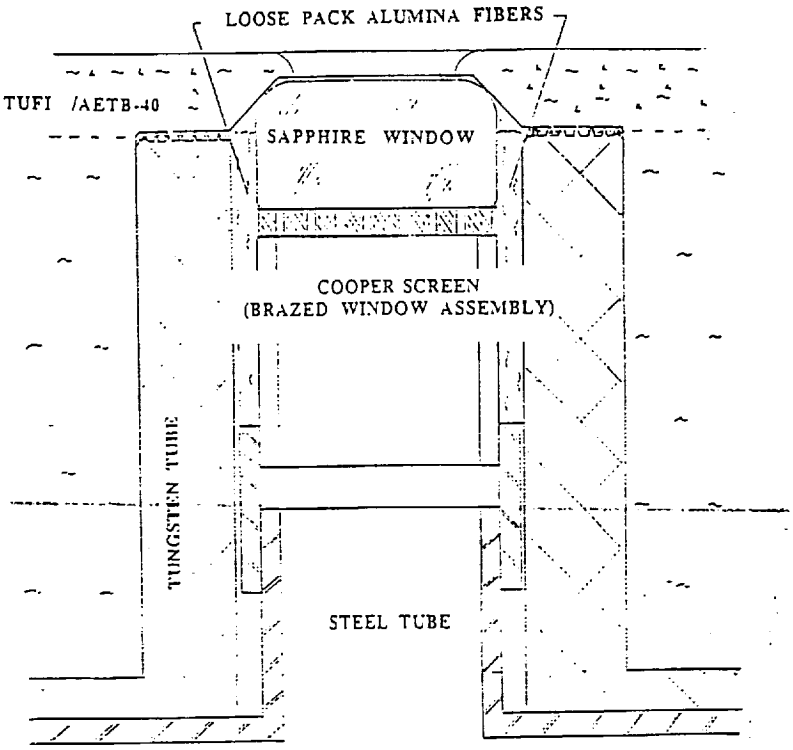

Figure P
Sketch of recommended RHE window design. Heat is transmitted to the copper element, a screen for larger diameters, and a washer for small diameters. The metal window holder is shielded from the shock region gases by overlapping the coating.

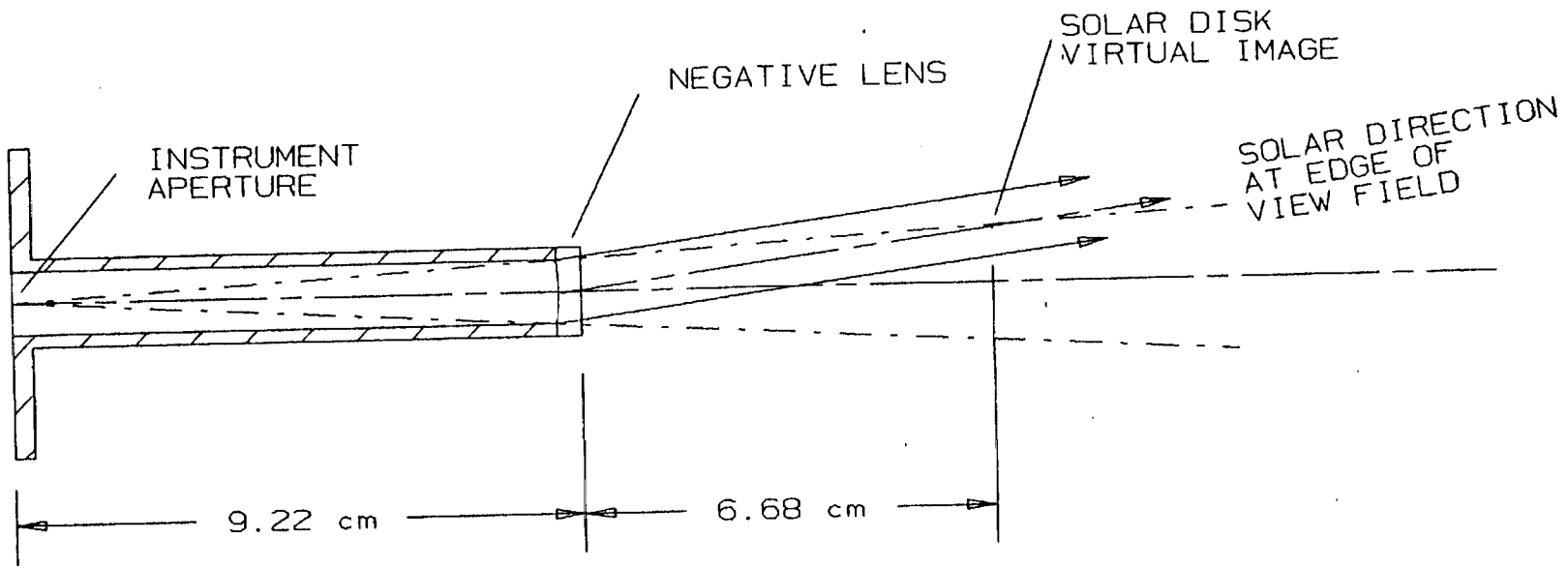

Figure Q

Sketch of a lens-apertured window based on AFE dimensional requirements. The viewfield in increased by shaping the inner surface of the window into a negative lens. A virtual image of the solar disk is formed within the field of view of the instrument aperture. The larger viewfield requirements for the solar calibrations is thereby accommadated.

APPENDIX - B

Spectral Measurements of Shock Layer Radiation in an Arc-Jet Wind Tunnel

Roger Craig
MCAT Institute
Moffett Field, California

Spectral Measurements of Shock Layer Radiation in an Arc-Jet Wind Tunnel

Giuseppe Palumbo,[1] Roger Craig[2] and Armando Carrasco[3]

KEY WORDS

Spectroscopic Analyzers, Optical Instrumentation, Radiation Instrumentation, Ultraviolet (UV) Instrumentation

ABSTRACT

Measurements were made of the radiating gas cap of a blunt body in an NASA-Ames 20MW arc-jet wind tunnel. The test gas was air. Spectra of the flux incident on a small aperture centered at the stagnation region were obtained. A helium-cooled, magnesium fluoride window transmitted flux into an evacuated collimating system that focused the aperture onto the entrance slit of a spectrometer. Data were obtained with films and by photomultipliers. ***The range covered was 120 nm*** to 1000 nm and the resolution was 0.05 nm to 0.5 nm. This paper presents preliminary results from the experiment. ***Representative spectral records from 200 nm to 1000 nm are shown.*** The spectra show the atomic lines from oxygen and nitrogen in the IR, as well as the molecular systems of NO, N_2, N_2^+, and CN. Copper, as a contaminant, and carbon are tentatively identified. Planned subsequent laboratory work will result in calibration of spectral sensitivity and refined wavelength determinations.

---

[1] Eloret Institute
Work performed under NASA Cooperative Agreement NCC2-653
1176 Maraschino Drive
Santa Clara, CA 94057

[2] MCAT Institute
Work performed under NASA Cooperative Agreement NCC2-762
NASA Ames Research Center
Moffett Field, CA 94035

[3] Thermo-Physics Facilities Branch
NASA Ames Research Center
Moffett Field, CA 94035

INTRODUCTION

Arc-jet wind tunnels, simulating conditions of high speed flight, are likely to be more and more important for aerospace research in the future. Computational modelling replacing the work of low speed wind tunnels, wherein real gas effects do not dominate, is becoming a reality. However, high speed flights, such as earth entry from a space mission (low earth orbit, LEO, or further), involves flowfield gases which are not in thermochemical equilibrium (references 1 and 2). This can include important levels of transport of radiative energy (reference 3). At present we cannot accurately predict the environmental conditions surrounding these spacecraft. Figure 1 shows flight regimes experienced for the entries of the Shuttle, Apollo and a proposed Aeroassisted Space Transfer Vehicle (ASTV). An ASTV is a conceptual vehicle which utilizes aerodynamic forces to decelerate and alter orbit parameters to rendezvous with the Shuttle or a space station (reference 1). The design of future, highly efficient heat-shields (i. e., not overdesigned) for these vehicles, and others, requires the capability of making accurate heating predictions. This fact is acknowledged by the inception of the Aeroassist Flight Experiment (reference 4). This experiment utilized a vehicle designed to be deployed and recovered by the Shuttle. It was to fly a trajectory which simulated an ASTV maneuver from geosynchronous earth orbit (GEO) to LEO for rendezvous with the Shuttle or a space station. The objective was to gather a data base for development of the ASTV and other advanced space transportation systems. The program was recently canceled due to funding limitations. Although the activity was cancelled the technical requirement remains.

Real gas computational models are being developed (reference 5) but validating data are lacking. Various models predict widely different radiative heating levels. ***For example, predictions of ASTV radiative heating from only the VUV atomic lines range from insignificant amounts to levels dominating the overall heating (references 6, 7 and 8).***

Arc-jet wind tunnels can produce the enthalpy and pressure conditions simulating these high speed entries. These facilities generally consist of an arc heater, a supersonic nozzle, a test box, a model holder and the necessary equipment to deal with the extreme heat transfer and the exhaust. Reference 9 describes arc-jet wind tunnels in some detail. In the past their main use has been for heat shield development. Future uses will include aerothermodynamic testing for spacecraft flight. Also these facilities can be used to conduct experiments to validate computational codes. Even though the size scale cannot

be simulated, a flow-field rich in non-equilibrated, radiating gas can be generated. Computational models can be exercised on arc-jet test conditions for comparison with experimental results. There are some major difficulties in this approach, however. The free stream plasma flow conditions (enthalpy, species distribution, energy states distribution, etc.) in an arc-jet are not well understood. Initial conditions for shock layer computational models can only be estimated. At present there are efforts to calculate the model test environments using computational models starting with the arc column, continuing with the conical or contoured expansion nozzle, and culminating in the flow field of a model located in the exit flow from the nozzle (reference 10). Experimental results are needed to support the theoretical work. A review of techniques used to study arc-jet wind tunnel flow is given in reference 11.

This paper reports on initial results of an arc-jet wind tunnel experiment. The experiment measured the spectral radiative flux emanating from the shock layer and incident on a blunt model placed in the supersonic stream. ***Data was taken from 120 nm to 900. This paper presents wavelength results from 200 to 900 nm. The VUV (120 nm to 200 nm) results will be reported on elsewhere.*** The purpose was to gather data to help characterize the stagnation region shock layer flow. Understanding this flow would be valuable for development and validation of advanced arc-jet wind tunnel design codes and help extend the capability of this class of facility to advanced aerothermodynamic testing.

The data shown in this paper are preliminary and do not benefit from final calibrations. The flux was spectrally resolved and over a wide range. The data will be analyzed and used to identify important radiating species and help determine the state of the gas and the operating characteristics of arc-jet wind tunnels.

EXPERIMENTAL SETUP

The experimental setup is as described in reference 12 except that the model diameter was increased to 6 inches. Figures 2 and 3 are from this reference and are included here. Figure 2 is a schematic plan view of the experiment. Supersonic flow from the arc is produced in the nozzle and the model is placed in the free stream. The standing shock layer over the model is indicated. Figure 3 is a schematic view of the model. The model face is a 6" diameter flat disk and the entire model is water cooled. A small aperture centered on the forward face admits the surface radiative flux. A helium cooled window, shown immersed in a cavity below the aperture, transmits the surface flux into the optical system. The optical system consists of a flat mirror, directing the

optical path to a concave mirror, which in turn collimates the beam to another concave mirror shown at the top of figure 2. This mirror focuses the aperture, via a flat turning mirror, onto the slit of the spectrograph. The spectrograph was a 0.5 meter instrument using a modified Czerny-Turner optical layout with the provision for operating either as a scanning monochromator or a film spectrograph . The portions of the system exposed to the plasma were all water cooled. Figure 4 shows the model arrangement in the test box. The nozzle exit can be seen at the left, and the aperture can be seen centered on the model face. The optical axis in front of the model was canted 15° from the centerline to reject radiation from the arc column.

TEST CONDITIONS

The test was conducted in the Ames 20 Megawatt Aerodynamic Heating Facility. The facility was operated with a supersonic nozzle with a 1.5 inch diameter throat and an 18" exit diameter. The facility operating parameters were as follows:

Test gas mixture: 80% air* and 20% Argon by mass,
arc current: 1000 amperes,
arc column pressure: 15psia,
nozzle pressure: 7.5psia,
test box pressure: 0.2 to 0.3 mm Hg, and
stagnation pressure: 9mm Hg.

The resulting free stream conditions for the present experiment is approximate as indicated in by the circle in figure 1. The velocity is deduced from an estimate of the free stream enthalpy which was, in turn, derived from the heating rate of a small sphere placed in the stream. It should be noted that the arc-jet free stream enthalpy, although repeatable, is not well characterized. Indeed, one of the objectives of this experiment is to help quantify this and other arc-jet wind tunnel performance characteristics.

Figure 5 is a photograph taken during a test. The shock is seen well formed over the flat model face. The intense radiation from the high temperature shock layer gases is clearly evident.

The experiment consisted of a series of 10 minute runs during each of which a specific spectral region was examined. The length of a run was limited by the heating loads on the test box. Data were obtained using film and

---

* Dried and filtered ambient air

photomultiplier tubes. The photomultiplier signal was processed with synchronous amplification. Readout was on a chart recorder and digitally recorded.

The instrument configurations used in the tests are summarized in Table 1.

DIGITAL DATA ACQUISITION

Four signals were recorded digitally during the experiment tests: stagnation pressure on the model face, ***optical system vacuum pressure***, photomultiplier high voltage, and photomultiplier output signal. The stagnation pressure, vacuum pressure, and the high voltage were recorded at one hertz with an analog mixer. The photomultiplier output signal was recorded at forty hertz.

Figure 6 shows the configuration of the data recording system for the time history of the pressure, vacuum, and high voltage signals. The system used a multiplexer and a controller configured with a portable personal computer. Twisted and shielded grounded cables were used to transmit the signals. The data acquisition and instrument control software were configured to record the data during each run at one hertz and concurrently display it on the monitor.

Figure 7 shows the configuration of the data recording system for the photomultiplier records. The system consisted of a controller, a scanning A/D converter, and a 16 channel isolated input rack connected to an NB-DMA board contained within the personal computer system. The data acquisition and control software was set to record at 40 Hertz.

The photomultiplier data presented here were manipulated for display purposes using graphic and analysis software.

RESULTS AND DISCUSSION

Computed Spectral Details.

The development of computational codes to predict the shock layer radiation, such as that measured by this experiment, is a parallel, ongoing activity at the Ames Research Center. These codes are based on calculations of the arc process, the expansion in the nozzle and the shock layer processes. The radiating shock region is very non-homogeneous and involves many kinetically controlled processes. Substantial radiation emanates from the nonequilibrated regions immediately behind the shock. Here the kinetic temperature is extremely high, approaching 50,000K. The spectral line radiation is strongly

Doppler broadened by this high temperature. The cooler parts of the shock will partially absorb the strong features directed toward the surface, but absorption will occur only at around the line centers because the absorption lines are narrow due to the low kinetic temperature. The surface radiative heating flux is thus seen to be the aggregate radiation from regions of very different conditions and estimates from computational codes involve consideration of complex interactive and kinetic processes. At present these codes exist as separate codes but the goal is to couple them together and validate the result as a reliable code for predicting arc-jet wind tunnel conditions. Figure 8 is a calculated spectrum. NO bands are seen from 190 nm to 300 nm. N2(2+) bands contribute energy from 280 nm on and merge with the stronger $N2^+$(1-) and N2(1+) bands which dominate the molecular systems from 300 nm to the infrared. Rich and diagnostically important atomic line radiation is predicted from oxygen and nitrogen in the infrared.

Test Results

As indicated above the data were taken with film and with photomultiplier tubes. The data presented herein are not corrected for instrument spectral response. This correction will be done with future work. The photomultiplier data was digitized in-situ. The film spectra density will be subsequently digitized.

Ultraviolet-visible results.

Data was acquired in the spectral region from 200 nm to 500 nm by both film and photomultiplier tube. Figure 9is a print from a film record taken on 8/10/92. The spectral range is from 330 nm to 450 nm. The uppermost spectrum is from the shock layer radiation and includes N_2^+(1-) $B^2\Sigma_u^+ - X^2\Sigma_g^+$ and CNv $B^2\Sigma - X^2\Sigma$ band systems and atomic lines from nitrogen and oxygen. The other spectra are mercury line calibrations. Figure 10 is a densitometer scan of the 360 nm to 395 nm region of figure M in which details of a portion of the N_2^+(1-) system are shown. The vib-rot structure can be seen in detail. This and the other film records will be digitally analyzed for subsequent use. Photomultiplier data were obtained in this region also. Figure 11 shows photomultiplier data of the spectral details from 200 nm to 300 nm. This spectral region is dominated by the NO_γ $A^2\Sigma^+ - X^2\Pi$ bands. Figure 12 is the photomultiplier data from 250 nm to 500 nm. These data were recorded digitally in-situ as well as with chart recorder backup. As with the VUV data, there is no correction to these figures to account for instrument spectral response. This correction awaits further laboratory work.

Visible-infrared results.

Noise limitations prohibited use of photomultiplier tubes beyond 700 nm. Film spectra, however, were obtained with great detail. Figure 13 is a print of the film taken from the 7/23/92 test. It covers the spectral range from 300 nm to 1000 nm with a resolution of approximately 0.1 nm. Figure 14 is a densitometer trace of this record. The details which overlap with the photomultiplier record can be seen. The important atomic oxygen and nitrogen emission lines are well resolved. Figure 15 is an densitometer trace of an expanded portion of this film indicating the resolution of the atomic lines. Several features await identification. Calibrations of the non-linearities of the film system will result in a data base allowing comparison of the intensities of these features with theoretical results. Their relative intensities will help understand the electron density of the plasma.

CONCLUSIONS

The spectra have been obtained from the flux incident on the stagnation surface of a flat model placed in the supersonic stream in an arc-jet wind tunnel. The preliminary data set shown is detailed at high resolution from 200 nm to 1000 nm. Important radiators are evident. The data set will be further developed and used to help refine and calibrate computational models of the aerothermodynamics of entry and of arc-jet wind tunnels.

ACKNOWLEDGMENTS

The authors wish to acknowledge the invaluable assistance of Brian Mifsud for Test Engineering support, Larry Hemstreet for integration and operation, Wendel Love for engineering support, Chul Park and Ellis Whiting for assisting development of the scientific aspects of the program, and Jaswinder Taunk for his help in developing the data acquisition system.

TABLE 1

I-TESTS USING FILM

Date	Grating Ruling, *l/mm*	Blaze Wavelength *nm*	Slit *microns*,	Exposure, *seconds*	λ range *nm*
7/8/92	60	300	20	100	200 to 500
7/15/92	180	150	20	60, 300	200 to 500
7/16/92	300	500	20	10, 50, 300	300 to 1000
7/23/92	300	500	20	100, 390	300 to 1000
7/24/92	1200	150	20	100, 600	200 to 400
8/10/92	1200	150	20	10, 100, 480	300 to 500

II-TESTS USING PHOTOMULTIPLIER TUBE

	Grating *l/mm*	Blaze *nm*	resolution, *nm*	spectral features	λ range, *nm*
8/4/92	2400	150	0.4	$N2^+(1-)$	300 to 500
8/4/92	2400	150	0.1	$N2^+(1-)$	300 to 500
8/5/92	2400	150	0.4	NO_γ	200 to 290
8/5/92	2400	150	0.1	NO_γ	200 to 290

11. Scott, Carl D., "Intrusive and Nonintrusive Measurements of Flow Properties in Arc Jets", Invited paper for the Workshop on Hypersonic Flows for Reentry Problems", co-organized by INRIA-Sophis Antipolis and GAMNI-SMAI, January 22-26, 1990, Antibes, France.

12. Palumbo, G., "Shock Layer Vacuum UV Spectroscopy in an Arc-Jet Wind Tunnel" NASA TM 02258, January, 1990.

FIGURES

Figure 1.
Flight regimes of mission returns for ASTV, Shuttle, and Apollo. The point indicated by the circle is an estimate of the altitude and velocity simulated by the arc-jet conditions used during the present tests.

Figure 2.
Schematic diagram of experimental setup. The arc column is to the left of the nozzle.

Figure 3.
Schematic diagram of model showing the aperture and window and orientation of the bow shock. Radiation incident onto the surface is reflected by the turning mirror to the concave mirror and thence to the spectrograph. Vacuum was maintained $<0.01\mu$ for the VUV tests.

Figure 4.
Photograph of model in test box. The optical system is protected by the water cooled coils shown as well as internal water cooling. The aperture can be seen in the face of the model. The nozzle exit can be seen at the left.

Figure 5.
Photograph of model during test. The stagnation shock is seen well formed over the model face and the intense radiation from the shock heated air is evident.

Figure 6.
Data acquisition system block diagram for recording the stagnation pressure on the model face, optical system vacuum pressure, photomultiplier high voltage.

Figure 7.
Data acquisition system block diagram for recording the photomultiplier output signal.

Figure 8.
Preliminary calculation of the spectral surface flux from the stagnation region of a model placed in an arc-jet wind tunnel.

Figure 9

Print from a film record taken on 8/10/92. The spectral range is from 330 nm to 450 nm. The uppermost spectrum is from the shock layer radiation and includes N_2^+(1-) $B^2\Sigma_u^+ - X^2\Sigma_g^+$ and CNv $B^2\Sigma - X^2\Sigma$ band systems and atomic lines from nitrogen and oxygen. The other spectra are mercury line calibrations.

Figure 10

Densitometer trace of the 360 nm to 395 nm region of the film record of figure M is shown. This region includes a portion of the N_2^+(1-) $B^2\Sigma_u^+ - X^2\Sigma_g^+$ band system. The vibration-rotation lines are seen to be well resolved. The atomic oxygen line at 394.8 nm is also shown.

Figure 11

Photomultiplier record of spectrum from 200 nm to 300 nm. This spectral region is dominated by the NO_γ $A^2\Sigma^+ - X^2\Pi$ bands.

Figure 12.

Photomultiplier record of spectrum from 250 nm to 500 nm. The molecular spectra from NO_γ $A^2\Sigma^+ - X^2\Pi$, N_2^+(1-) $B^2\Sigma_u^+ - X^2\Sigma_g^+$ and CNv $B^2\Sigma - X^2\Sigma$ are in this region as well as atomic lines from oxygen and nitrogen and copper (contamination from the arc electrodes).

Figure 13.

Photographic print of 7/23/92 film spectrum from 300 nm to 1000 nm. Two different duration exposures of the shock layer emission were taken. Exposure A is a short exposure of emission from the shock layer and an overlapping calibration exposure from a Hg lamp. Exposures B and D are Hg lamp calibration exposures. Exposure C is a long exposure without overlapping Hg lamp calibration. Selected Hg emission lines in the first, second and third orders, are indicated.

Figure 14.

Densitometer trace of 7/23/92 film spectrum from 500 nm to 1000 nm. The important atomic oxygen and nitrogen emission lines are well resolved. Also seen are the copper lines at 324.7 nm and 327.4 nm in the second and third orders.

Figure 15.

Expanded portion of the 7/23/92 film spectrum densitometer trace showing the atomic lines near between 800 nm and 880 nm. Several features await identification.

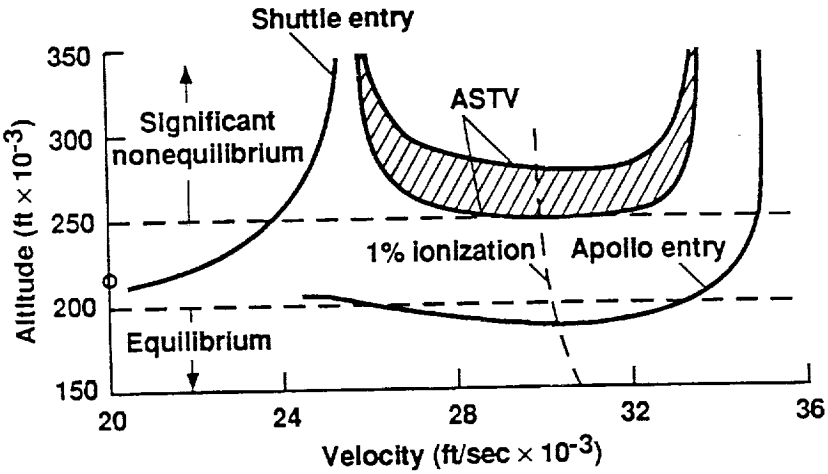
Shuttle entry
350
300
250
200
150
Altitude (ft × 10^-3)
Significant nonequilibrium
ASTV
1% ionization
Apollo entry
Equilibrium
20
24
28
32
36
Velocity (ft/sec × 10^-3)

Palumbo-1

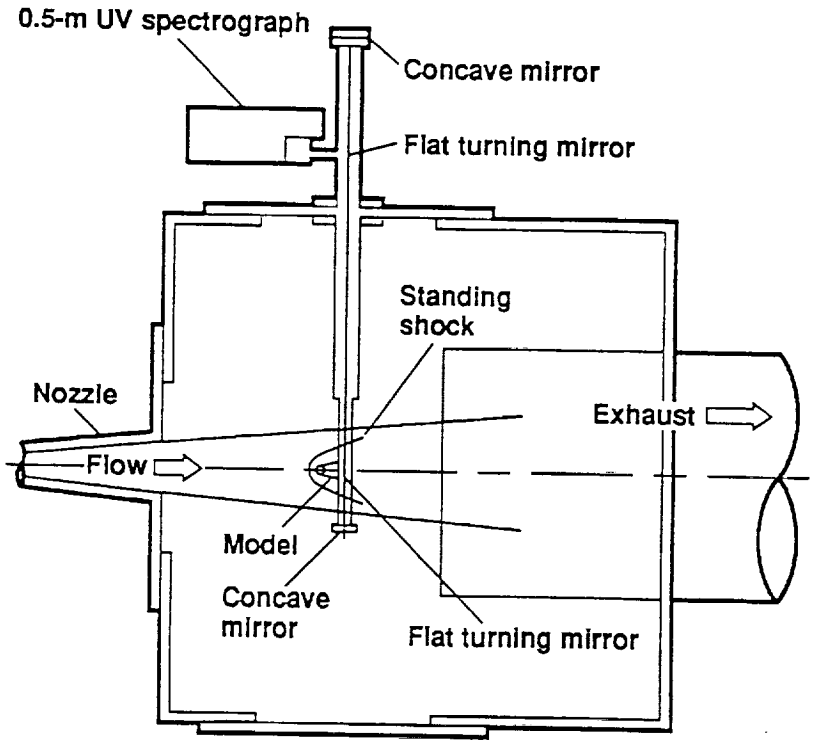
0.5-m UV spectrograph
Concave mirror
Flat turning mirror
Standing shock
Nozzle
Exhaust
Flow
Model
Concave mirror
Flat turning mirror

Palumbo-2

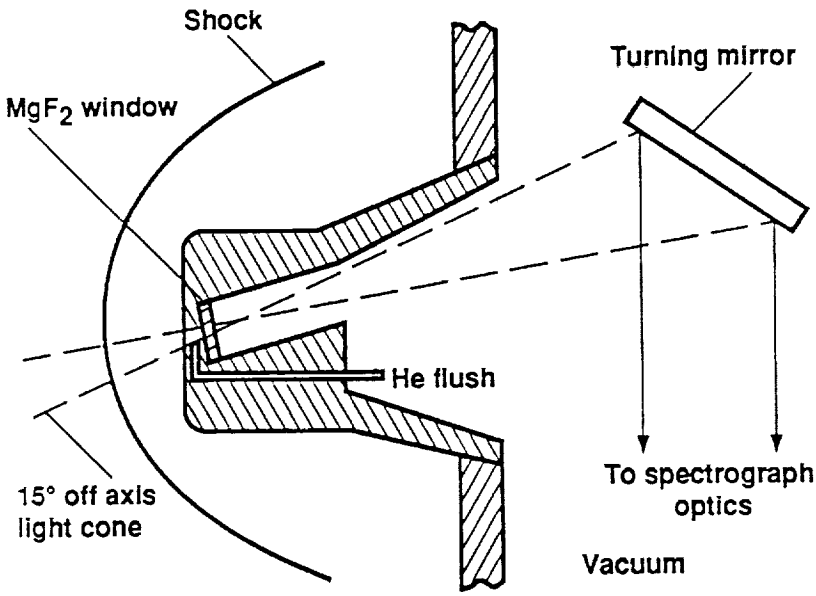
Shock
MgF_2 window
Turning mirror
He flush
15° off axis
light cone
To spectrograph
optics
Vacuum

Palumbo-3

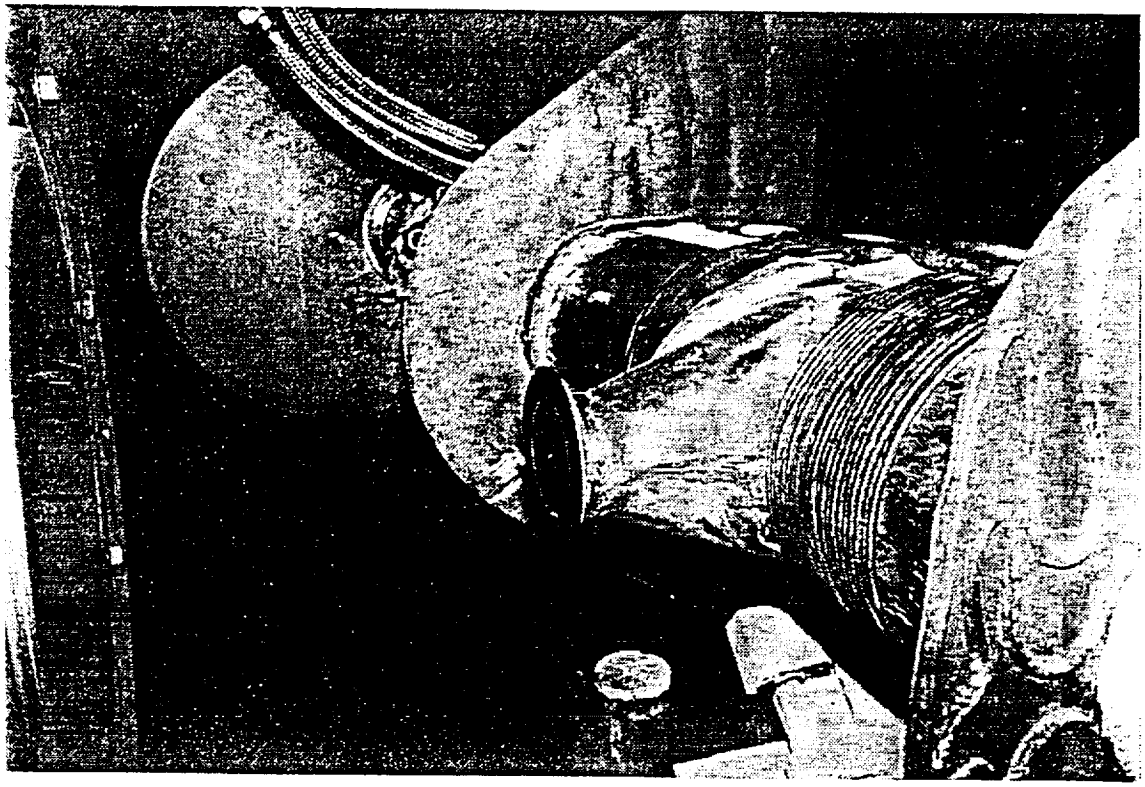

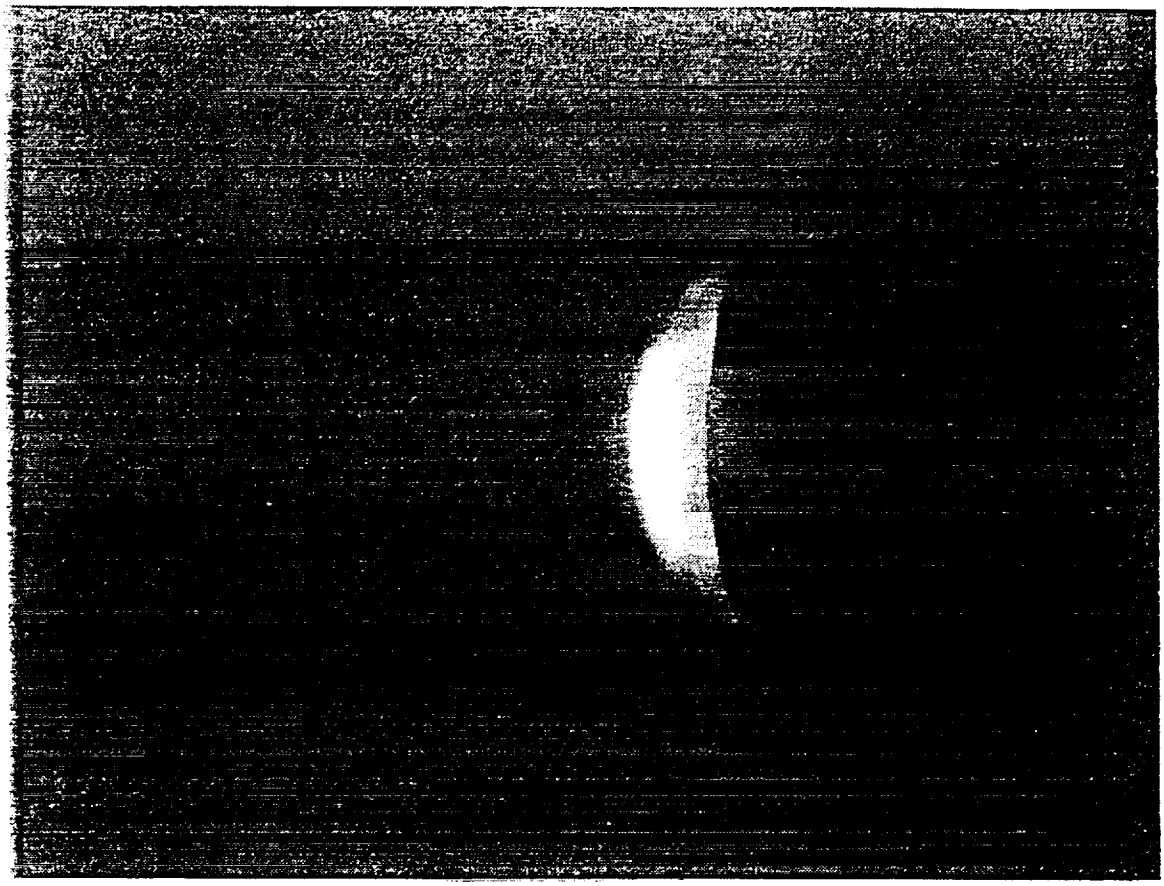

5

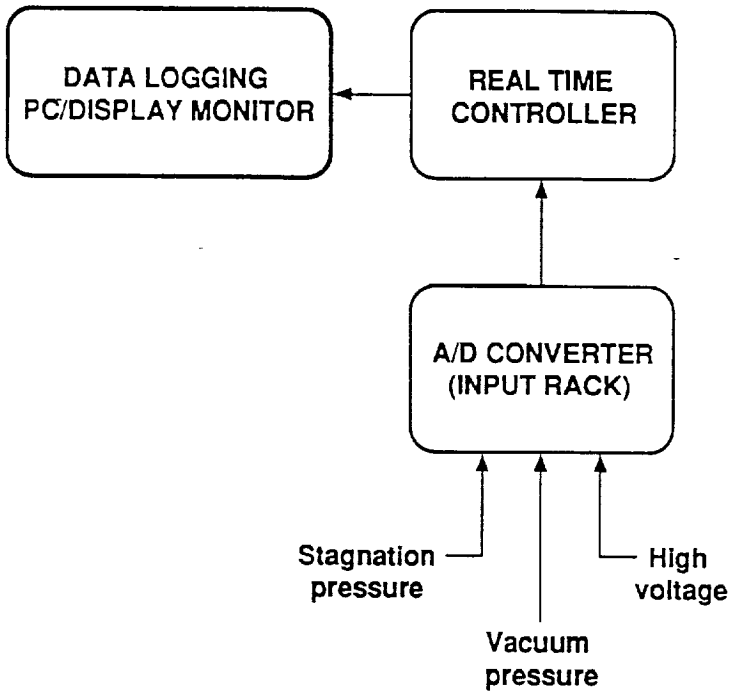
DATA LOGGING
PC/DISPLAY MONITOR
REAL TIME
CONTROLLER
A/D CONVERTER
(INPUT RACK)
Stagnation
pressure
Vacuum
pressure
High
voltage

Palumbo-6

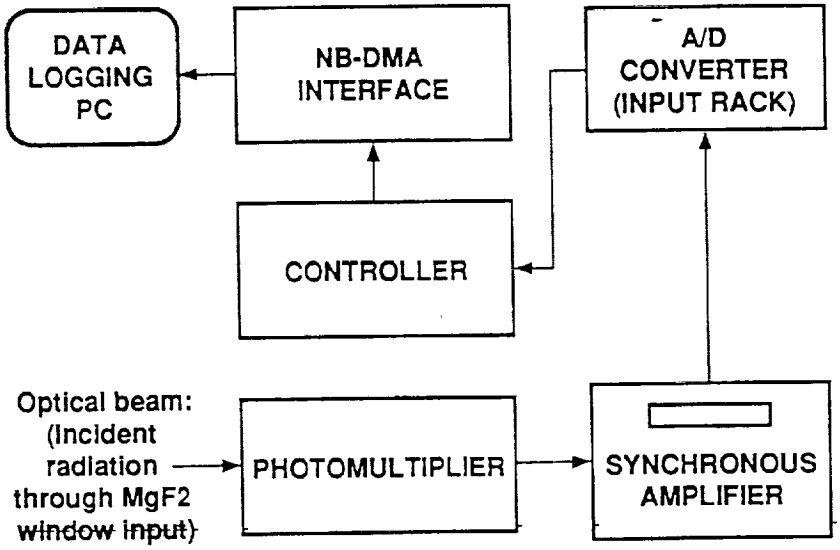
DATA LOGGING PC
NB-DMA INTERFACE
A/D CONVERTER (INPUT RACK)
CONTROLLER
Optical beam: (Incident radiation through MgF2 window input)
PHOTOMULTIPLIER
SYNCHRONOUS AMPLIFIER

Palumbo-7

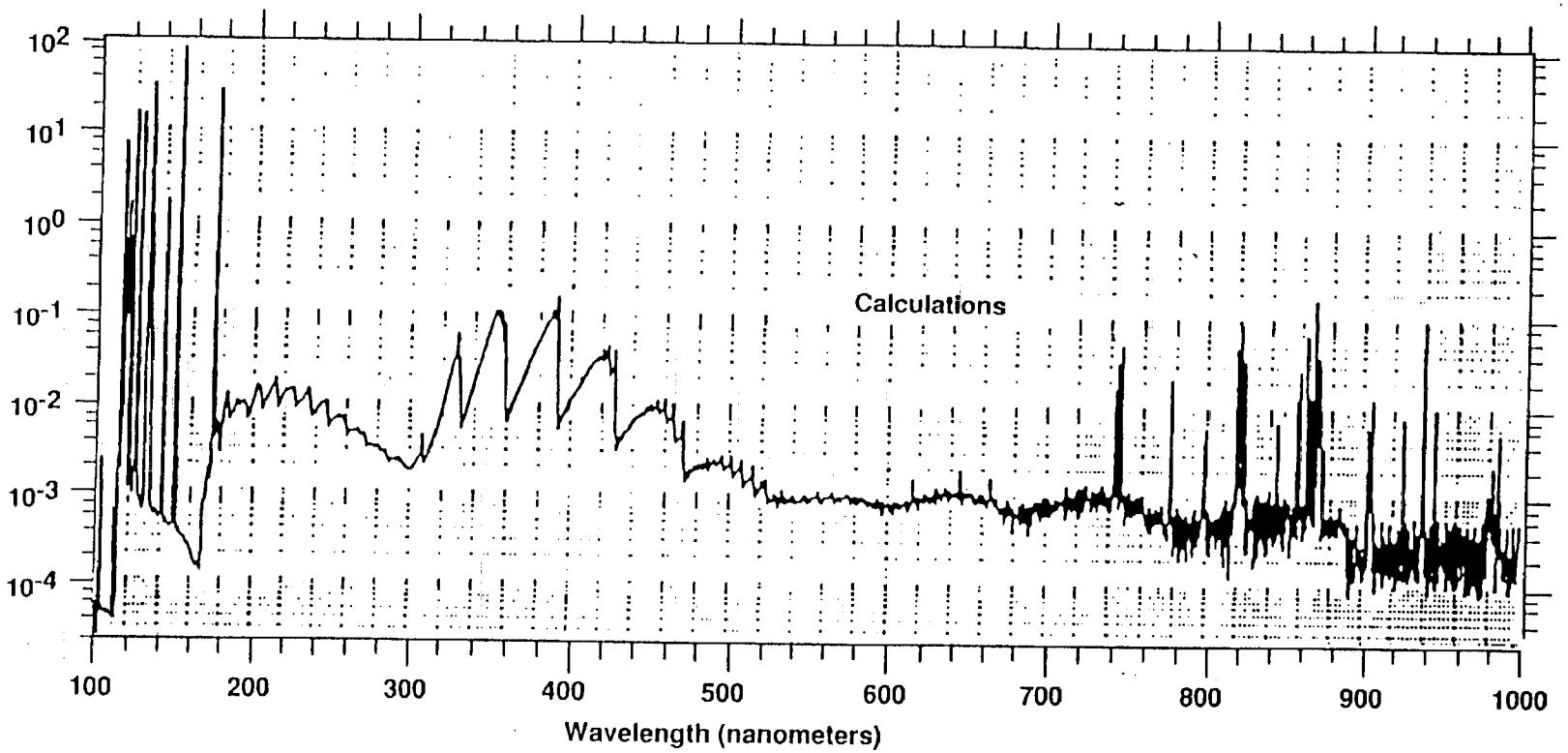
10^2
10^1
10^0
10^{-1}
10^{-2}
10^{-3}
10^{-4}
Calculations
100
200
300
400
500
600
700
800
900
1000
Wavelength (nanometers)

Palumbo-8

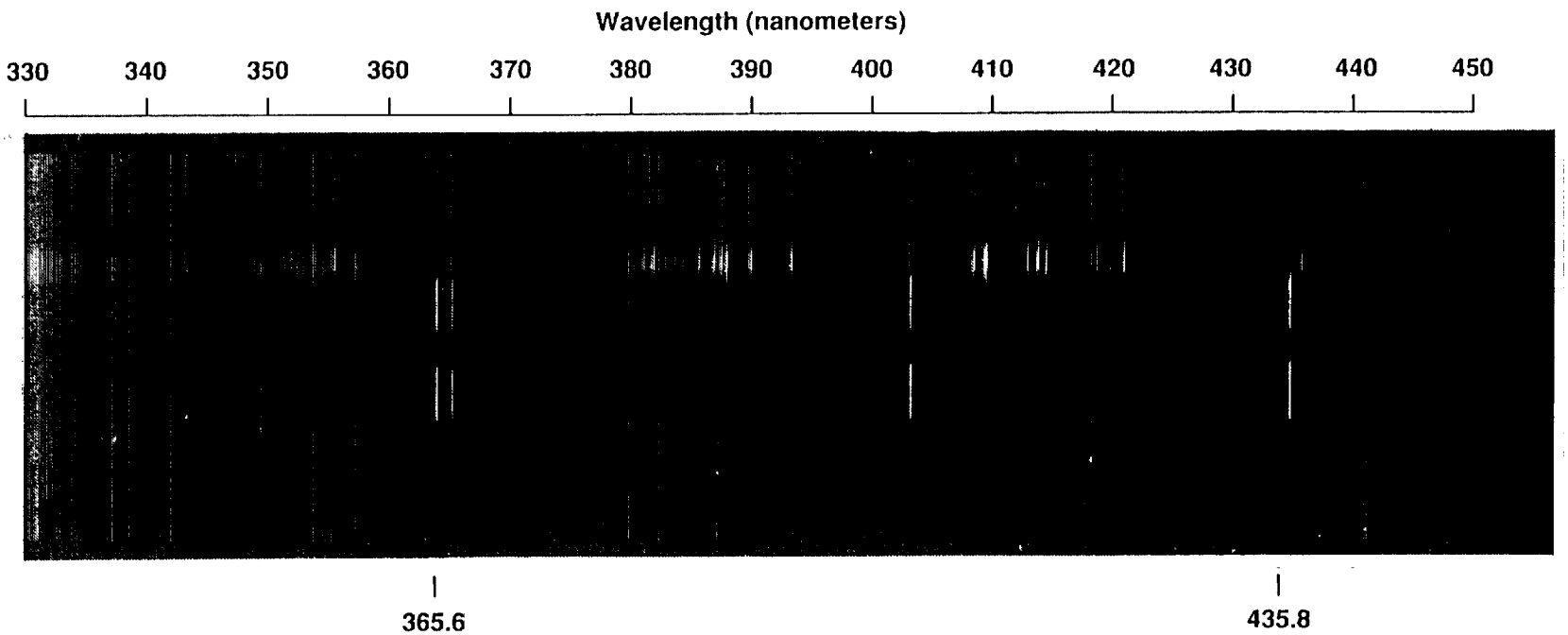
Wavelength (nanometers)
330
340
350
360
370
380
390
400
410
420
430
440
450
365.6
435.8
Hg lines

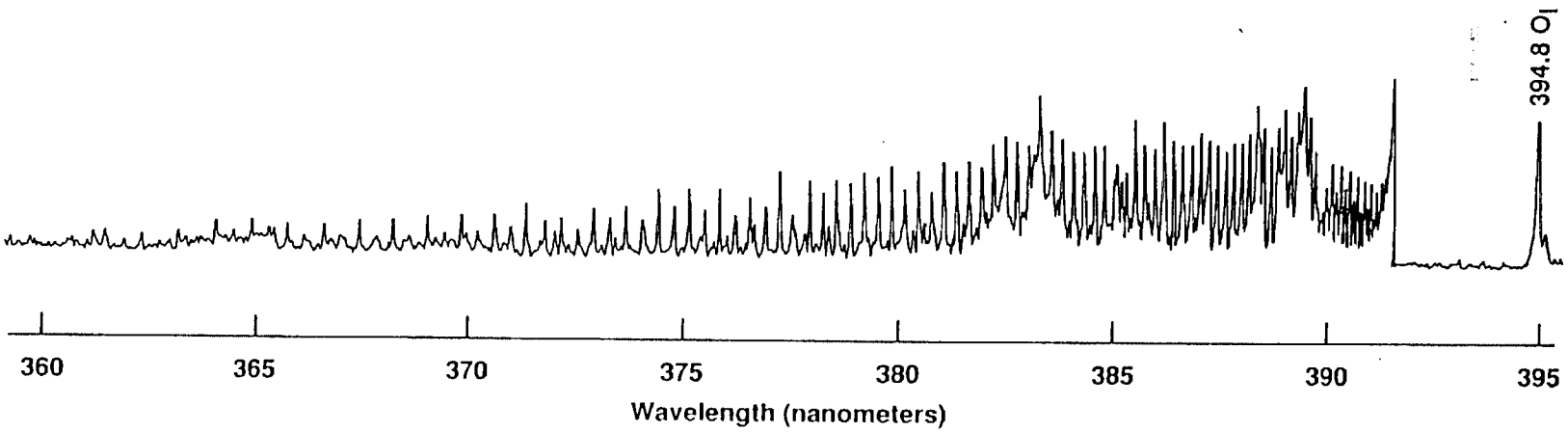
394.8 O I
360
365
370
375
380
385
390
395
Wavelength (nanometers)

Palumbo-15 / 0

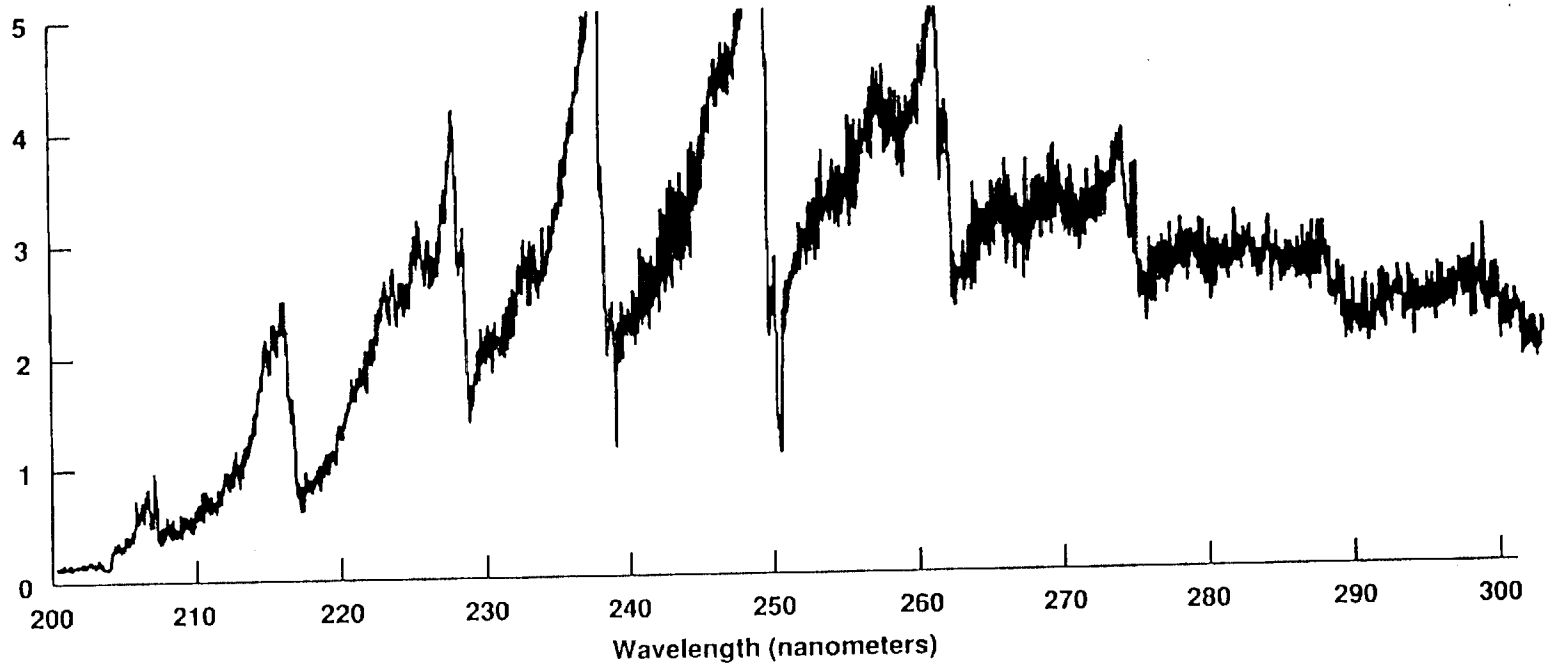
5
4
3
2
1
0
200
210
220
230
240
250
260
270
280
290
300
Wavelength (nanometers)

Palumbo-☞ //

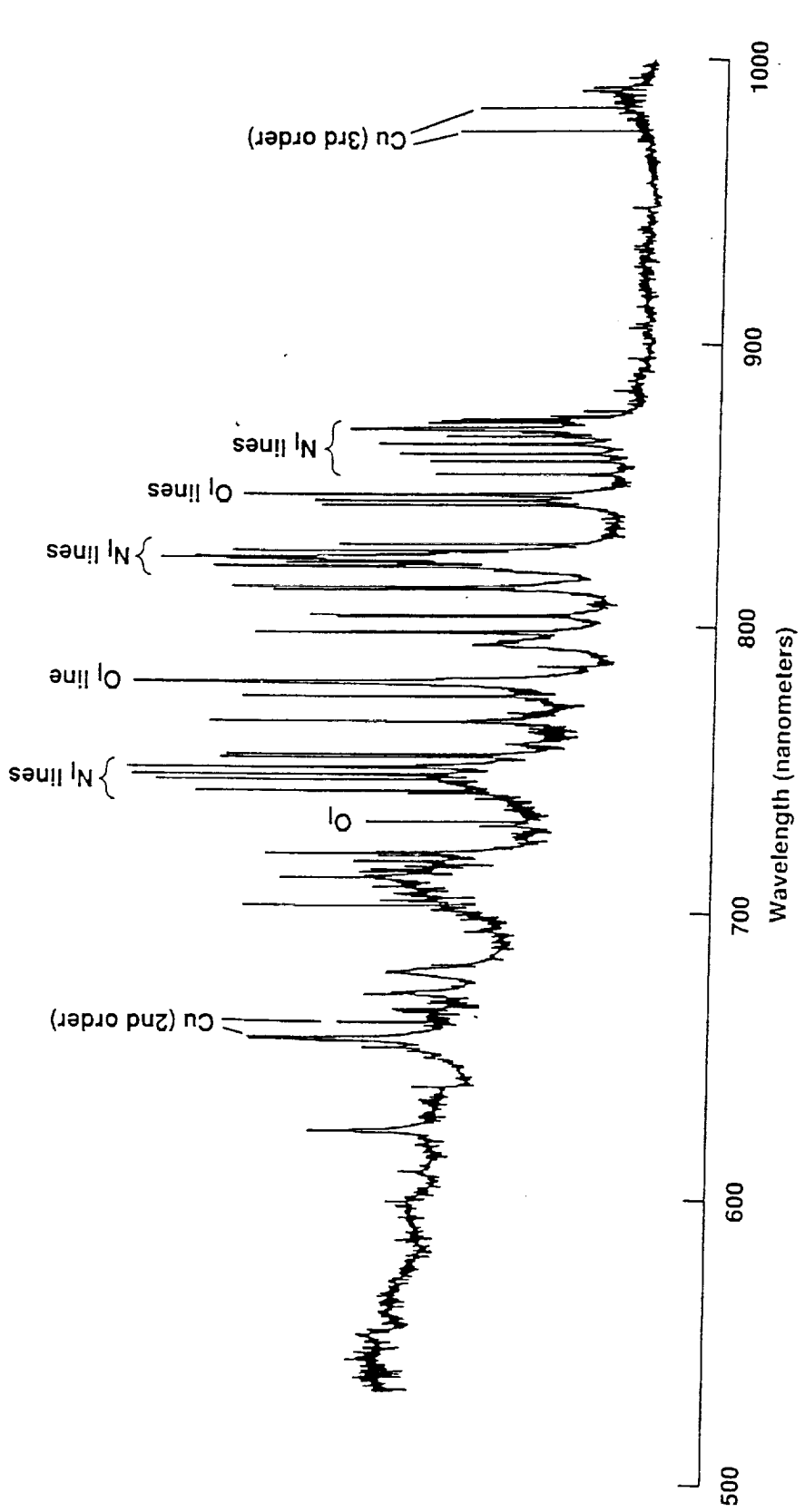

Palumbo 12-14

12-13

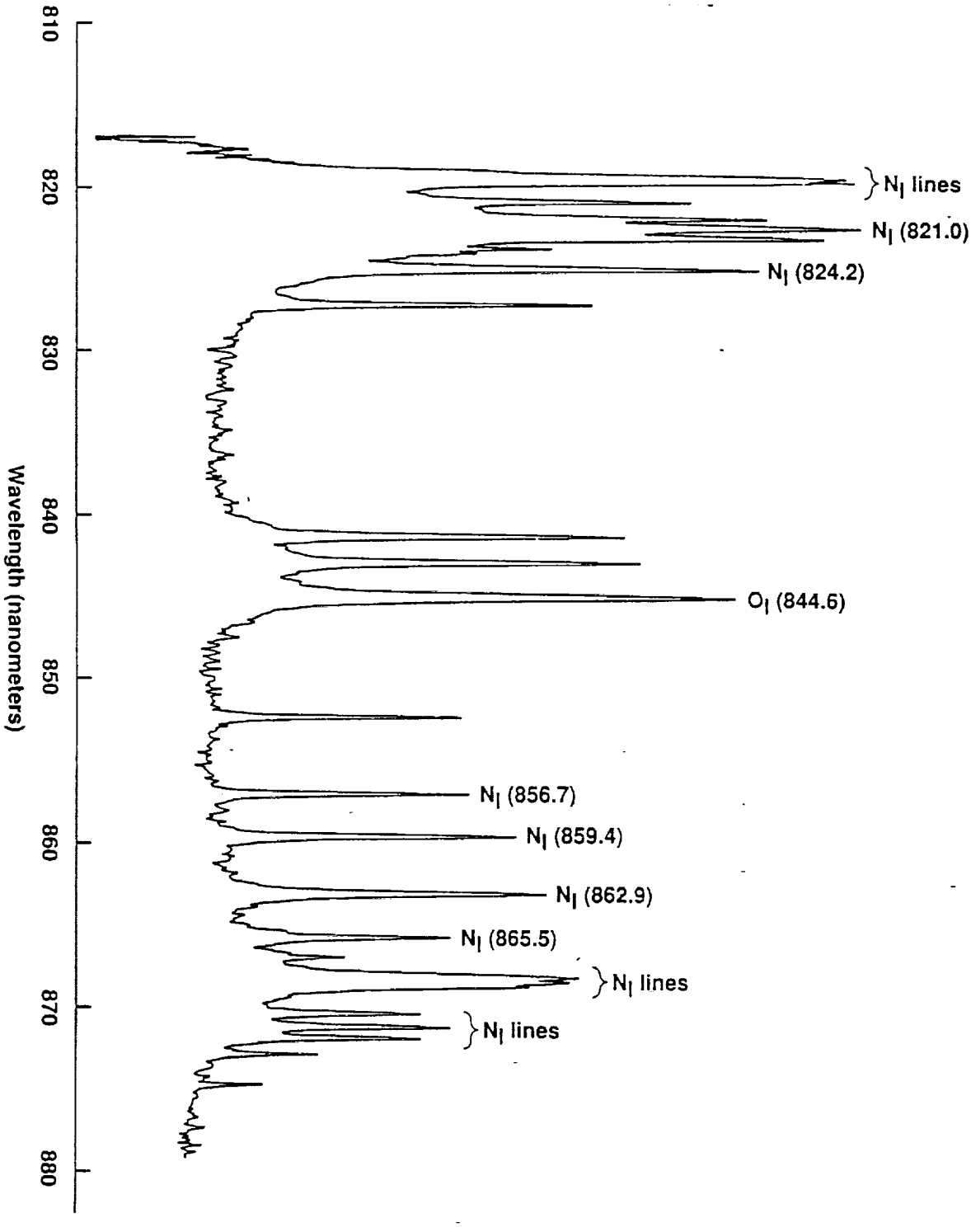
810
820
830
840
850
860
870
880
Wavelength (nanometers)
N I lines
N I (821.0)
N I (824.2)
O I (844.6)
N I (856.7)
N I (859.4)
N I (862.9)
N I (865.5)
N I lines
N I lines

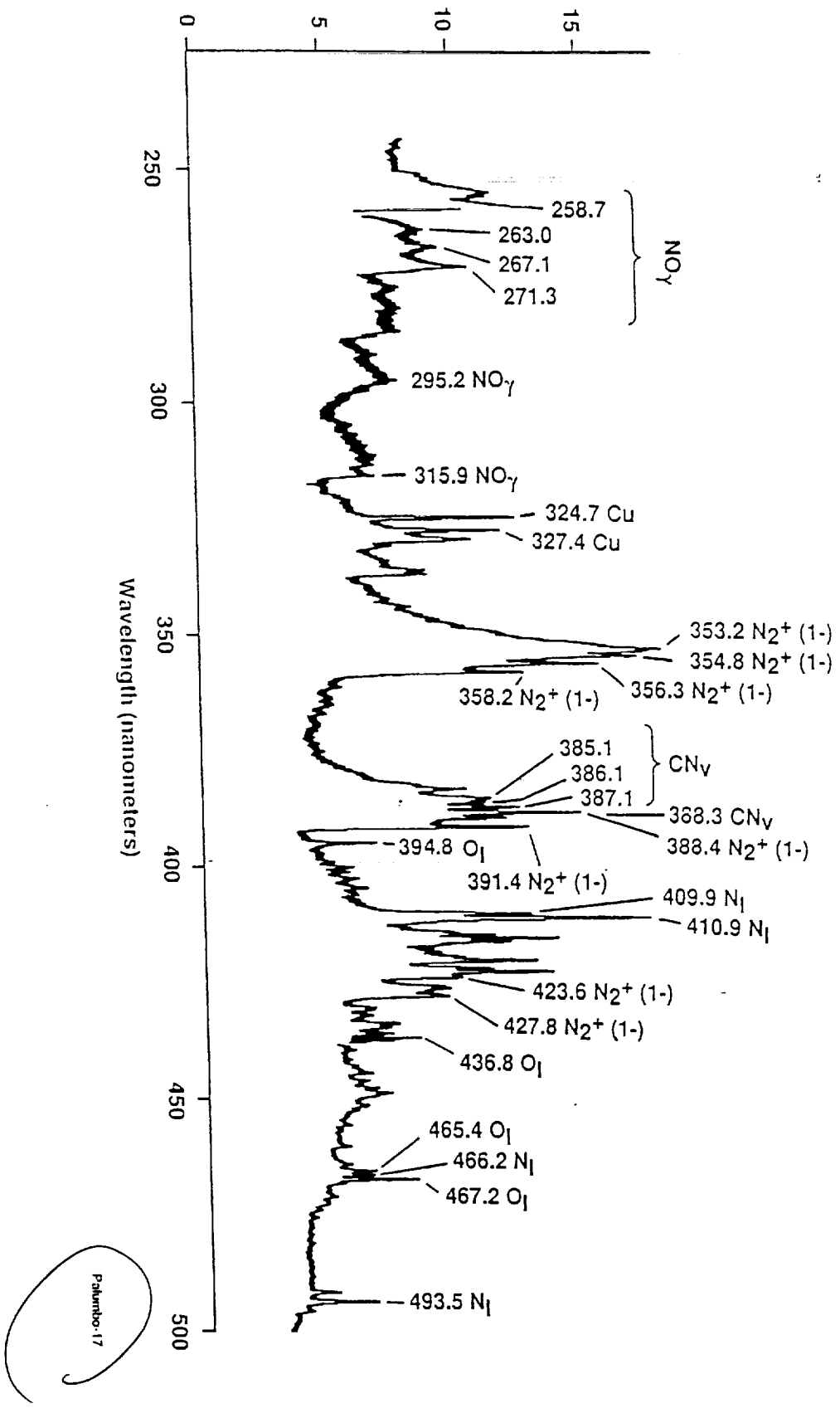

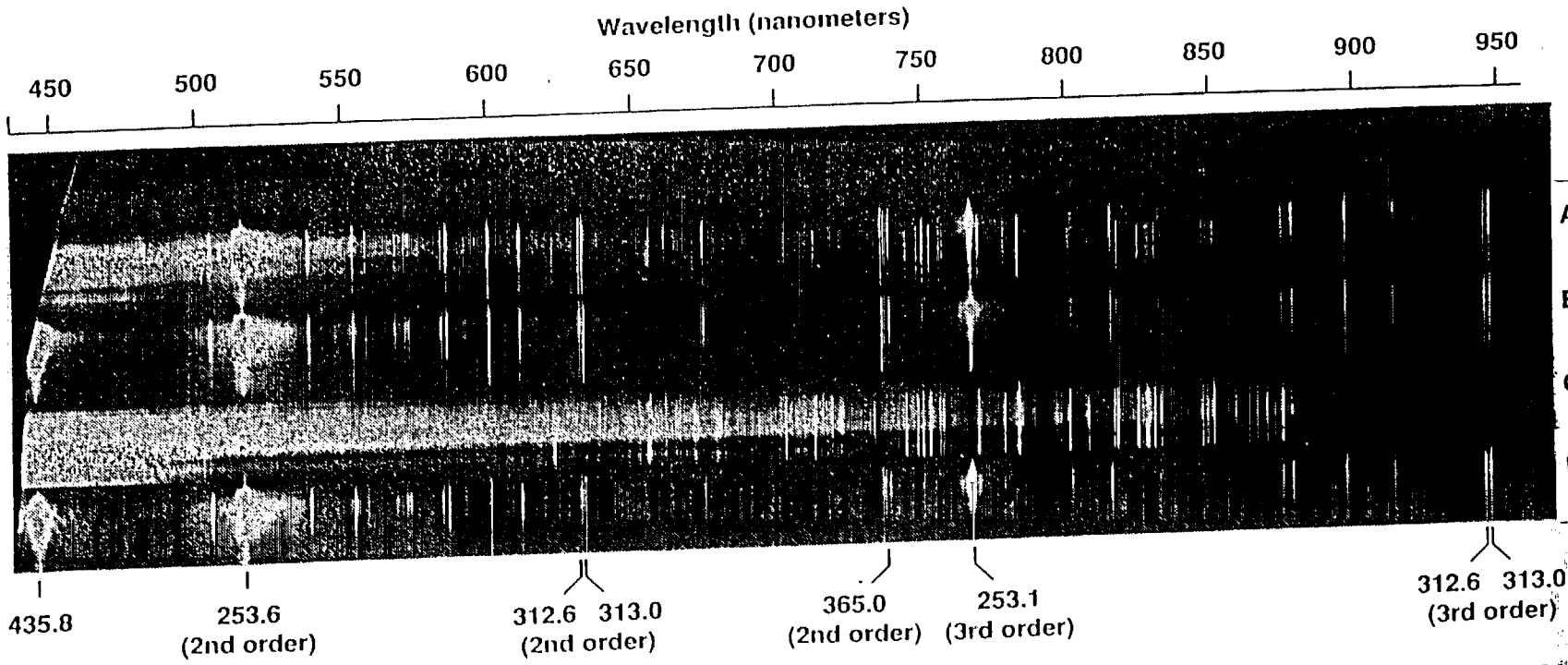

Hg lines

394.8

APPENDIX - C